Quaternary Science Reviews 218 (2019) 137–156

Contents lists available at ScienceDirect

Quaternary Science Reviews

journal homepage: www.elsevier.com/locate/quascirev

Refining the Late Quaternary tephrochronology for southern South America using the Laguna Potrok Aike sedimentary record

Rebecca E. Smith [a, *], Victoria C. Smith [a], Karen Fontijn [b, c], A. Catalina Gebhardt [d], Stefan Wastegård [e], Bernd Zolitschka [f], Christian Ohlendorf [f], Charles Stern [g], Christoph Mayr [h, i]

[a] Research Laboratory for Archaeology and the History of Art, 1 South Parks Road, University of Oxford, OX1 3TG, UK
[b] Department of Earth Sciences, University of Oxford, OX1 3AN, UK
[c] Department of Geosciences, Environment and Society, Université Libre de Bruxelles, Belgium
[d] Alfred Wegener Institute, Helmholtz Centre for Polar and Marine Research, Am Alten Hafen 26, D-27568, Bremerhaven, Germany
[e] Department of Physical Geography, Stockholm University, SE-10691 Stockholm, Sweden
[f] University of Bremen, Institute of Geography, Geomorphology and Polar Research (GEOPOLAR), Celsiusstr. 2, D-28359, Bremen, Germany
[g] Department of Geological Sciences, University of Colorado, Boulder, CO, 80309-0399, USA
[h] Institute of Geography, Friedrich-Alexander-Universität Erlangen-Nürnberg, Wetterkreuz 15, 91058 Erlangen, Germany
[i] Department of Earth and Environmental Sciences & GeoBio-Center, Ludwig-Maximilians-Universität München, Richard-Wagner-Str. 10, 80333 München, Germany

ARTICLE INFO

Article history:
Received 12 March 2019
Received in revised form
29 May 2019
Accepted 2 June 2019

Keywords:
Quaternary
Tephrochronology
Volcanic ash
Geochemistry
Stratigraphy
South America
Patagonia
PASADO
Lacustrine

ABSTRACT

This paper presents a detailed record of volcanism extending back to ~80 kyr BP for southern South America using the sediments of Laguna Potrok Aike (ICDP expedition 5022; Potrok Aike Maar Lake Sediment Archive Drilling Project - PASADO). Our analysis of tephra includes the morphology of glass, the mineral componentry, the abundance of glass-shards, lithics and minerals, and the composition of glass-shards in relation to the stratigraphy. Firstly, a reference database of glass compositions of known eruptions in the region was created to enable robust tephra correlations. This includes data published elsewhere, in addition to new glass-shard analyses of proximal tephra deposits from Hudson (eruption units H_1 and H_2), Aguilera (A_1), Reclus (R_1, $R_{2\text{-}3}$), Mt Burney (MB_1, MB_2, MB_x, MB_{1910}) and historical Lautaro/Viedma deposits. The analysis of the ninety-four tephra layers observed in the Laguna Potrok Aike sedimentary sequence reveals that twenty-five tephra deposits in the record are the result of primary fallout and are sourced from at least three different volcanoes in the Austral Andean Volcanic Zone (Mt Burney, Reclus, Lautaro/Viedma) and one in the southernmost Southern Volcanic Zone (Hudson). One new correlation to the widespread H_1 eruption from Hudson volcano at 8.7 (8.6–9.0) cal ka BP during the Quaternary is identified. The identification of sixty-five discrete deposits that were predominantly volcanic ashes (glass and minerals) with subtle characteristics of reworking (in addition to three likely reworked tephra, and one unknown layer) indicates that care must be taken in the analysis of both visible and invisible tephra layers to decipher their emplacement mechanisms.

1. Introduction

The nature and scale of past volcanism, and how this varies relative to external forcing, must be established in order to devise adequate hazard and risk assessments. This study focusses on the analysis of the lacustrine sediment record of Laguna Potrok Aike, in southern South America (Fig. 1). This sediment sequence likely preserves tephra from explosive eruptions of the arc volcanoes in the southernmost sector of Chile. The postglacial eruptive history of these volcanoes has been derived by integrating proximal records with those preserved in other lacustrine records (e.g., Stern, 2008; Weller et al., 2018). However, due to issues in preservation, little is known about volcanism prior to deglaciation and following the Last Glacial Maximum (LGM; e.g., Fontijn et al., 2014). The sedimentary record of Laguna Potrok Aike is therefore ideal to investigate Late Quaternary volcanism as it lies downwind of major productive

* Corresponding author.
E-mail address: rebecca.smith@seh.ox.ac.uk (R.E. Smith).

https://doi.org/10.1016/j.quascirev.2019.06.001

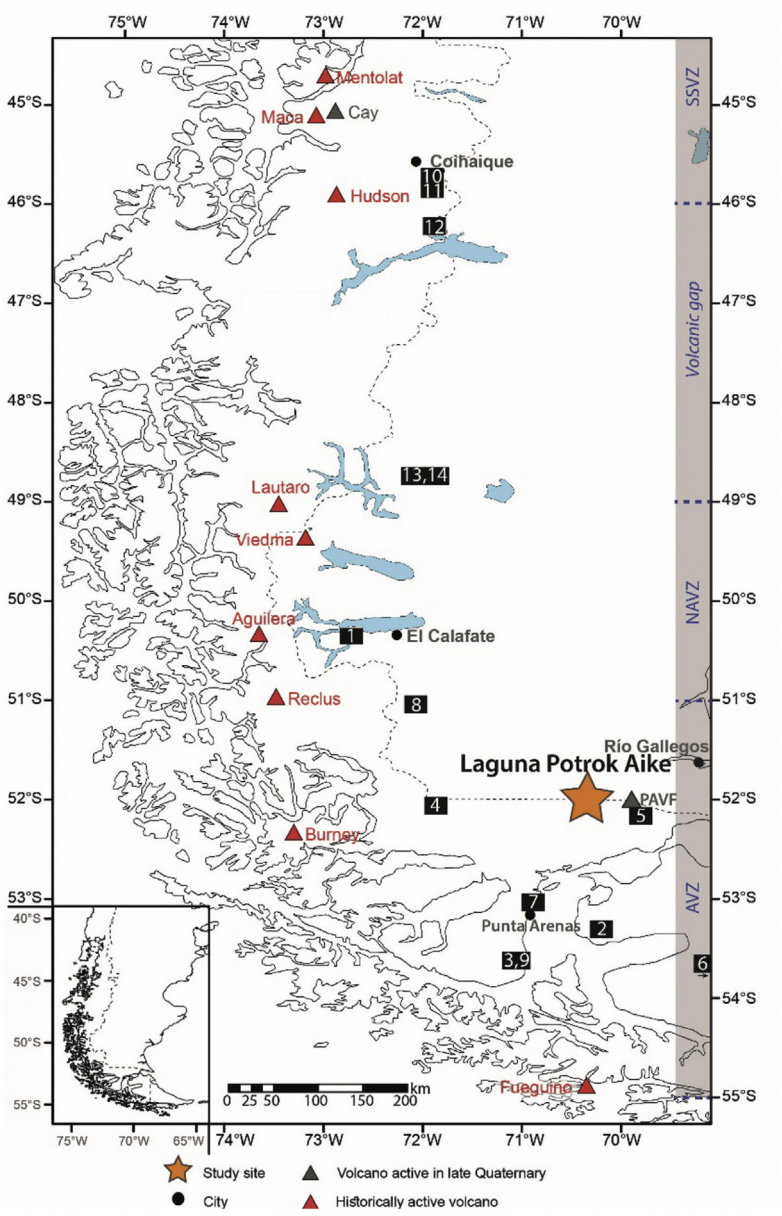

Fig. 1. Map of southernmost South America with active volcanoes of the Austral and southernmost Southern Volcanic Zones. Star shows study site, Laguna Potrok Aike. White numbers in black boxes indicate the locations of terrestrial tephra samples (see Table 1). Abbreviations in blue text with grey shaded background to the right of map demark the volcanic zones; AVZ = Austral Volcanic Zone; NAVZ = northern Austral Volcanic Zone; SSVZ = southern Southern Volcanic Zone (as per Stern, 2004). (For interpretation of the references to colour in this figure legend, the reader is referred to the Web version of this article.)

volcanic centres, was not glaciated during the last glacial period and thus provides an ~80 ky record of volcanism (Coronato et al., 2013; Gebhardt and Ohlendorf, 2019). Reconstructing a long-term record of volcanism from this region will additionally allow us to test the possible influence of external factors on volcanic activity; for example, the relationship between climate and volcanic activity (e.g., Rawson et al., 2016). Various studies have suggested that the removal of ice load after deglaciation affects the generation, storage and eruption of magma (e.g., Jellinek et al., 2004; Nowell et al., 2006; Rawson et al., 2016; Sigvaldason et al., 1992; Watt et al., 2013).

1.1. Records of volcanism in southernmost South America

Andean volcanoes are divided into zones, and this paper focuses on the Southern Southern Volcanic Zone (SSVZ; 41.5–46°S; Stern, 2004) where Hudson volcano is located, and the Austral Volcanic Zone (AVZ; 49–55°S; Stern, 2004, Fig. 1). The AVZ contains several large and frequently active volcanoes, including Mt Burney, Reclus, Viedma, Lautaro and Aguilera, which are located ~200 km, ~250 km, ~350 km, ~390 km, ~300 km from Laguna Potrok Aike, respectively. Several thick ash layers from these centres have been observed in sedimentary archives across southern South America, including H_1 from Hudson at 7.57–7.85 cal ka BP, R_1 from Reclus at 14.37–15.26 cal ka BP, MB_1 from Mt Burney at 8.85–9.95 cal ka BP, and A_1 from Aguilera at 3.07–3.34 cal ka BP (all dates from Stern, 2008).

There is a relatively good understanding of the large volcanic eruptions that have dispersed tephra widely across the southernmost part of South America during the Holocene (e.g., Del Carlo

et al., 2018; Naranjo and Stern, 2004; Stern, 2008; Stern et al., 2015; Wastegård et al., 2013; Weller et al., 2014, 2015, 2017, 2018). However, beyond the Holocene, relatively little is known regarding the regional eruptive history. This is because long records of environmental change and terrestrial deposits are typically poorly preserved as a result of ice advance and retreat during the LGM, in addition to persistently strong westerly winds in the area which easily remove tephra from the landscape (e.g., Fontijn et al., 2014).

Further study of tephra deposits in the southern hemisphere could greatly improve the scope for correlating records over wide areas (including for example, South America and Antarctica). This would better refine the chronology of both climatic and volcanic events. Recent work demonstrates that tephra layers from southern Andean volcanoes exist far beyond South America. For example, a tephra from Sollipulli volcano (Alpehué pumice, So-A horizon) in the Chilean Lake District has been identified in sub-Antarctic South Georgia at ~3000 km distance from the source (Oppedal et al., 2018), and widespread tephra layers from Mt. Burney (MB_1) and Reclus (R_1) volcanoes have been identified in the Falkland Islands (Monteath et al., 2019; both centres are ~950 km away). Koffman et al. (2017) have additionally investigated cryptotephra deposits found in surface snow and shallow firm samples from the West Antarctic Ice Sheet (WAIS) Divide Camp, Antarctica and correlated these to the AD 2011 Puyehue-Cordón Caulle eruption in Chile. Narcisi et al. (2012) have also produced correlations between Andean volcanic centres and ash identified in Antarctica, but some of these are brought into question by Del Carlo et al. (2018).

Bulk chemical analysis of southernmost South American tephra deposits is currently the most widely-used analytical method for characterising volcanic deposits and distinguishing source-localities (e.g., Stern, 2008; Weller et al., 2014, 2015, 2017). However, the analysis of volcanic ash deposits using individual chemical fingerprinting of glass-shards is increasingly recommended since it precludes the analysis of minerals, which can vary in abundance with distance from the vent (Tomlinson et al., 2015). In addition, the variation in melt composition is very sensitive to variations in crystallisation, which in particular varies between eruptive units, and data from bulk compositional analysis is not as effective as determining these often very subtle changes as individual glass-shard chemistry. As such, the chemistry of individual grains of glass provides the most accurate approach to fingerprint the composition of the deposit across wide areas and subsequently permits a robust source allocation and tephrocorrelations (e.g., Del Carlo et al., 2018; Fontijn et al., 2016; Tomlinson et al., 2015). For these reasons, the chemical fingerprinting of glass-shards from proximal deposits (Section 3.1) and the subsequent refinement of compositional fields has been undertaken to facilitate robust tephra correlations between volcanic centres and chemically analysed deposits from the Laguna Potrok Aike sedimentary archive (Tables 2 and 3; Figs. 4 and 5).

This study focuses on the volcanic deposits in the 106.09 m-composite depth (m-cd) sediment sequence from site 2 of the ICDP expedition 5022 (5022-2CP) 'Potrok Aike Maar Lake Sediment Archive Drilling Project' (PASADO; Zolitschka et al., 2006). The site of Laguna Potrok Aike has not been covered by the Patagonian ice sheet during or after its Middle Pleistocene formation at ~0.77 Ma (Zolitschka et al., 2006). The sediment record recovered in the framework of the ICDP-PASADO mission spans the last ~80 ka, and therefore provides a record of part of the last glacial period and the Holocene (Gebhardt and Ohlendorf, 2019). It is subsequently the most comprehensive and longest record of volcanism in southern South America yet studied, offering the best opportunity to analyse regional volcanic activity during the Late Quaternary.

The tempo of activity and composition of the melts erupted may additionally provide insights into the relationship between ice-unloading and the occurrence of explosive volcanic activity (e.g., Huybers and Langmuir, 2009; Fontijn et al., 2016; Rawson et al., 2015; Rawson et al., 2016; Watt et al., 2013). In areas where decompressional melting plays an important role in primary melt production, such as Iceland and mid-Ocean ridges, an increase in volcanic activity has been suggested as a result of deglaciation (e.g., Jellinek et al., 2004; Jull and McKenzie, 1996; Crowley et al., 2015). In continental arcs like the Andes, where primary magma production is less likely to be influenced by cycles of glaciation (e.g., Watt et al., 2013), such cycles are thought to instead influence magma storage and residence time in the crust (e.g., Rawson et al., 2016; Watt et al., 2013). This is based predominantly on the principle that the longer the melt sits in the crust, the more evolved it becomes because of fractional crystallisation (Rawson et al., 2016; Watt et al., 2013).

Geochemical analysis of glass-shards in a high-resolution study using deposits from Mocho-Choschuenco volcano in the Chilean Lake District enabled the identification of three phases of post-glacial volcanic activity (Rawson et al., 2015, 2016). Here, relatively low frequency, large magnitude, silicic eruptions were recorded between 1 and 5 kyr after the termination of the last glaciation, during the first phase; the second phase comprised of medium-frequency, small-magnitude events of mafic composition; the final phase consisted of high-frequency events that varied in magnitude, and were predominantly of intermediate composition (Rawson et al., 2016). Rawson et al. (2016) hypothesised that significant changes in the eruption magnitude and composition of magmas at Mocho-Choshuenco are due to storage and release, which is most likely a response to changes in ice-overburden. This hypothesis can be better tested with synglacial records such as that from Laguna Potrok Aike.

1.2. Laguna Potrok Aike and previous tephra work

Laguna Potrok Aike (51°58′S, 70°23′W) is situated in the Pali Aike Volcanic Field (PAVF), related to back-arc volcanism of southern South America (Fig. 1). The lake is located downwind from the major productive centres of the SSVZ and AVZ, and thus Laguna Potrok Aike is an ideal site for the deposition of tephra from these centres (Wastegård et al., 2013).

During previous investigations of the Laguna Potrok Aike sedimentary record, 18 visible tephra layers were chemically characterised (Wastegård et al., 2013), allowing correlation between different sites due to identification of the MB_1 and R_1 tephra units. An increased abundance of tephra was identified between 72-38 and 25-19 cal ka BP (Wastegård et al., 2013; ages adjusted to reflect new age-model by Gebhardt and Ohlendorf, 2019). Not all of the identified tephra were chemically analysed in the previous study, and therefore we revisit the record to carry out more detailed analyses and increase the number of eruptions possibly recognised.

This new study significantly adds to prior research on the site and in the region as it:

1) provides new glass-chemistry for proximal deposits of the Austral Volcanic Zone, enabling more robust and compatible correlations to volcanic centres;
2) identifies five new primary ashfall (tephra) layers in the Potrok Aike record, providing a more complete regional tephra record for the region;
3) includes individual glass-shard geochemistry for each tephra layer in the Potrok Aike sequence with sufficiently large glass-shards;
4) identifies reworked ash layers, which provide insights into the palaeoenvironment for the last ~80 kyr, and

5) provides a dataset to test the relationship between tephra frequency and composition as well as changes in climate relating to ice-unloading.

2. Methods

2.1. Terrestrial tephra samples from the Austral Volcanic Zone

Terrestrial tephra samples were obtained from 14 sites across southernmost South America (Fig. 1 and Table 1). These samples had previously been analysed for bulk chemical composition and the sources of these tephra layers were already established and in most cases published (Table 1). However, because bulk chemical compositions cannot easily be compared with individual grain glass-shard chemical compositions, the glass-shards were analysed using techniques described in Section 2.3.2.

2.2. Chronology of Laguna Potrok Aike sequence

The chronology for this lake sequence is from Gebhardt and Ohlendorf (2019) who used radiocarbon dates, Infrared Stimulated Luminescence (IRSL) measurements, known eruptive ages for tephra deposits, and tuning of relative palaeointensity between Laguna Potrok Aike and the Sint-800 stack to produce an updated age-depth model for the Laguna Potrok Aike sedimentary sequence.

2.3. Visible tephra layers from Laguna Potrok Aike

Visible tephra layers were collected from the sedimentary sequence, taking care to avoid core-ends, using a scalpel. All tephra layers are referred to as LPA_m-cd with the composite depth (cd) quoted in metres and representing the uppermost boundary of the horizon.

2.3.1. Visual analysis of glass-shards and/or minerals

The samples were analysed under a binocular microscope to evaluate the relative abundance of:

- glass-shards
- organic material
- detrital material

Glass-shard morphology, angularity (Fig. 2), and colour were also described. The dominant minerals present were additionally noted, including whether minerals predominantly had preserved or degraded glass-coatings. These data (in addition to chemical analyses; Section 2.3.2) were used to provide detailed further information on the depositional nature and help distinguish between primary or reworked events (e.g., McLean et al., 2018; Supplementary File 2).

Notably, the distinction between primary and reworked tephra layers was determined using a point-based criteria. Points relate to indicators of reworking, and deposits which had three or more points relating to reworking characteristics were considered as reworked. Before concluding the classification, these deposits were also considered as a whole afterwards (e.g., appearance in lithology, including contact, and previous reports on layer). The criteria that were used are as follows, and deposits received one point for each of these features identified:

- minerals in the sample are rounded or sub-rounded;
- minerals have no glass coating, or glass-coating is degraded;
- glass-shard abundance is low ($\leq$60%);
- high abundance of organic material ($\geq$5%);
- high abundance of detrital material ($\geq$10%);
- chemistry of glass-shards is the same as those in the tephra layer/s below.

2.3.2. Compositional analysis of glass-shards

Tephra samples from terrestrial environments were gently crushed with a pestle and mortar before being wet-sieved using 80 μm nylon mesh and demineralised water. Visible tephra samples from pelagic sediments were wet-sieved using 25 μm nylon mesh and demineralised water; organics and minerals were removed from the tephra samples, and then glass-shards were isolated using heavy liquid density separation techniques as per Blockley et al. (2005) to extract components with densities between 2.0 g cm^3 and 2.5 g cm^3. Glass-shards were subsequently mounted in Epoxy resin stubs, which were sectioned and polished to expose a flat surface, before being carbon coated for chemical analysis.

The major element composition of glass-shards was analysed at the Research Laboratory for Archaeology and the History of Art, University of Oxford, using a wavelength-dispersive JEOL JXA-8600 electron microprobe (EMP) equipped with four spectrometers, and an accelerating voltage of 15 kV. Shards were predominantly analysed with a low beam current of 6 nA and a 10 μm beam diameter; very small shards were analysed with a 5 μm beam, and a 4 nA current. Thirty shards were analysed for each sample where possible.

Sodium (Na) was analysed first to minimise element loss due to migration. Elemental peaks were collected for a total of 60 s (P), 50 s (Cl), 40 s (Mn), 30 s (Si, Ca, K, Al, Ti, Fe, Mg), or 12 s (Na) and for half of the total peak time on each of the background positions on either side of the peak. Prior to analysis, the EMP was calibrated for each element using primary mineral standards. To verify the calibration, Max Planck Institute reference glasses (MPI-DING) were used as secondary standards; StHs6-80/G, ATHO-G, and GOR132-G (Jochum et al., 2006) were analysed at the beginning, during and at the end of all sample runs. The averaged values of these lie within two standard deviations of the preferred values (see Jochum et al., 2006).

Preferable total values for unknown samples are $\geq$95–100.5 wt% (e.g., Shane, 2000; Lowe, 2011; Fontijn et al., 2016). To maximise the retention of analyses where devitrification has started to occur, lower total values of >94–100.5 wt% are considered acceptable (Shane, 2000; Fontijn et al., 2016). Micro-phenocrysts, vesicles and resin were avoided during analyses. To account for variable secondary hydration, data were normalised to 100 wt%. Individual glass-shard chemical analyses are shown as biplots, particularly using SiO_2/K_2O, as potassium is the most distinguishing element of SVZ and AVZ deposits due to along-arc variations in the potassium composition of the melt (Kilian et al., 2003; Stern, 2008; Wastegård et al., 2013).

3. Results

3.1. Glass chemical composition of proximal deposits

The commonly used bulk tephra (whole-rock) X-ray fluorescence method is not particularly appropriate for fingerprinting tephra and confirming correlations in tephrochronology. To resolve this issue, glass-shards from widespread regional markers (H_1, H_2, MB_1, MB_2, R_1, and A_1) were analysed to produce a database of individual glass-shard major element chemistry (Tables 1 and 2). Existing glass-chemical data for proximal samples by Del Carlo et al. (2018) and those affiliated to historical Lautaro and Viedma eruptions from Mayr et al. (2019) were additionally used for comparison (Fig. 3).

Table 1
Widespread tephra samples analysed in this study.

Volcano	Marker horizon	Label	Site	Location	Archive	Thickness (cm)	Reference	Previous geochemical analysis	Reference in Fig. 1
Aguilera	A_1	93–03	Lago Roca	50°22′S, 72°45′W	Bog peat	10	Stern (2008)	Bulk and glass EMPA major elements/Trace elements	1
Burney	MB_2	90–16	Altos de Boqueron (TDF)	53°17′S, 70°10′W	Bog peat	2	Stern (1992); Stern (2008)	Bulk trace elements	2
	MB_2	93-07(-2)	Lago Parillar	53°26′S; 71°05′W	River sediment	4	Stern (2008)	Bulk trace elements	3
	MB_1	BF-370cm	Rio Rubens	52°02′S, 71°57′W	Barking Fox bog core	10	Markgraf (pers comms) in Stern (2008)		4
	MB_1	Laguna Tom Gold	Laguna Tom Gold (TG1)	52°09′S, 69°56′W	Site excavation	5–10	Massone (1989); Stern (2008)	Bulk trace elements	5
	MB_1	93-21W	Chico river (TDF)	53°33′S, 68°42′W	Bog peat	1	Stern (2008)		6
	MB_1	Unknown 4							NA
Reclus	R_1	90–06	Pampa Alegre (Rio Seco)	53°04′S, 70°51′W	Fluvial-glacial sediment	6	Stern (1992); Stern (2008)	Bulk trace elements	7
	R_1	R1-RioTurbio	Rio Turbio	51°S, 72°W	River sediment	Unknown	Unreported		8
	R_1[a]	90–01	Rio Tres Brazos (PB)	53°16′S, 71°02′W	Bog peat	1	Stern (1992); Stern (2008)	Bulk trace elements	9
	R_1	Unknown 1							NA
	R_1	Unknown 2							NA
	R_1	Unknown 3							NA
Hudson	H_2	H2_Q_60-85	Lago Quijada	45°43′S, 71°54′W	Lacustrine sequence	24 - Table 1 Weller et al. (2015)	Weller et al. (2014), 2015	Bulk trace elements	10
	H_2	H2_E_0-30	Lago Espejo	45°52′S, 72°1′W (Chile)	Lacustrine sequence	53 - Table 1 Weller et al. (2015)	Weller et al. (2015)	Bulk trace elements	11
	H_1	93-21G	Chico River (TDF)	53° 33′S, 68°42′W	Bog peat	20	Stern (2008)		6
	H_1	RI-16II	Río Ibáñez, Aisén	46°19′S, 71°54′W	River sediment	Unknown	Stern (2008)		12
Lautaro		VT_1 (AD 1959/60?)	Laguna Verde	49°20′S; 72°98′W	Lacustrine sequence	5	Mayr et al. (2019)	Glass EMPA major elements	13
		VT_2 (AD 1933?)	Laguna Verde	49°20°S; 72°98′W	Lacustrine sequence	3			13
		VT_3 (AD 1876/78?)	Laguna Verde	49°20°S; 72°98′W	Lacustrine sequence	6			13
		VT_4 (AD 1536–1669)[b]	Laguna Verde	49°20°S; 72°98′W	Lacustrine sequence	1			13
		GT_2 (AD 1959/60?)	Laguna Gemelas	49°39′S; 72°90′W	Lacustrine sequence	4			14
		GT_3 (AD 1876/78?)	Laguna Gemelas	49°39′S; 72°90′	Lacustrine sequence	5			14
Viedma?		GT_1 (AD 1963/1964?)	Laguna Gemelas	49°39′S; 72°90′W	Lacustrine sequence	5			14

[a] R_1 - 90-01 was reported as A_1 (Aguilera) in Stern (2008), but this was a geochemically unconfirmed correlation.
[b] Extrapolated age.

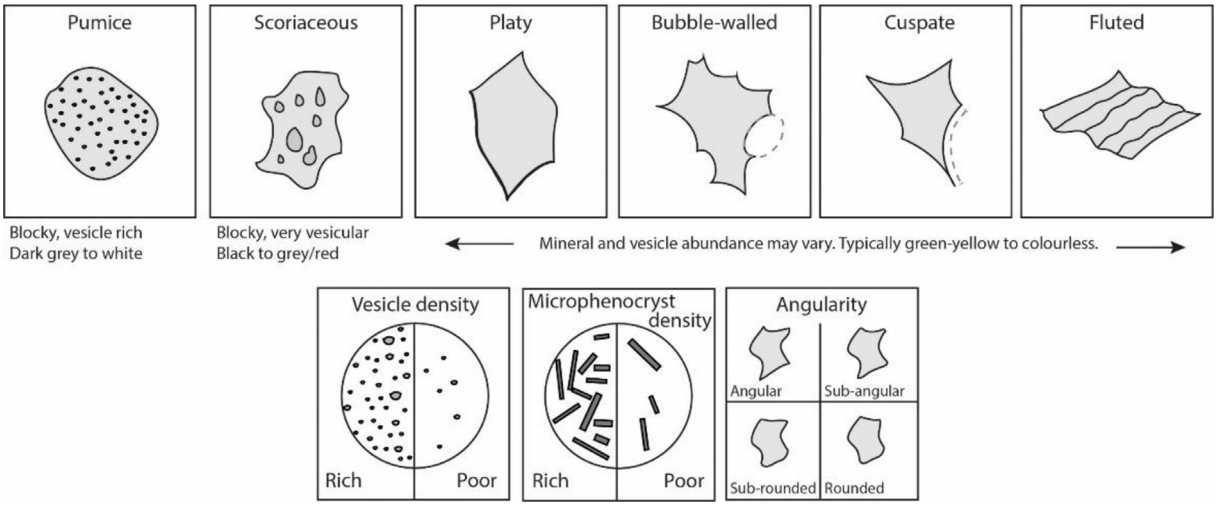

Fig. 2. Illustration of glass-shard morphologies identified. The angularity description is used for minerals. The relative abundance of shards (not shown) is derived from Terry and Chilingar (1955).

Table 2
Average glass-shard geochemistry for widespread eruptions normalised to 100%[a] (all data is from this study, except Lautaro/Viedma reported by Mayr et al., 2019). Total represents analytical total. Dataset presented in Supplementary File 1.

Volcano	Marker	SiO_2	TiO_2	Al_2O_3	FeOt	MnO	MgO	CaO	Na_2O	K_2O	P_2O_5	Cl	Total
Hudson	**H1**	***n = 53***											
	avg	63.72	1.24	16.12	4.81	0.15	1.49	3.02	6.08	2.83	0.38	0.15	98.30
	stdev	0.58	0.06	0.19	0.30	0.05	0.14	0.26	0.18	0.13	0.05	0.04	1.75
	H2	***n = 29***											
	avg	69.02	0.70	15.18	2.95	0.11	0.63	1.61	5.88	3.62	0.12	0.18	97.30
	stdev	0.35	0.05	0.20	0.16	0.05	0.08	0.17	0.22	0.08	0.03	0.03	1.98
Aguilera	**A1**	***n = 24***											
	avg	77.12	0.15	12.62	0.98	0.03	0.17	1.01	3.57	4.14	0.02	0.19	97.53
	stdev	0.30	0.03	0.15	0.10	0.03	0.03	0.07	0.21	0.09	0.02	0.03	1.08
Burney	**MB1**	***n = 52***											
	avg	76.07	0.28	13.09	1.56	0.04	0.37	1.84	4.79	1.68	0.05	0.23	96.39
	stdev	1.69	0.14	0.42	0.47	0.03	0.15	0.25	0.24	0.19	0.04	0.04	1.50
	MB2	***n = 10***											
	avg	76.70	0.24	13.03	1.28	0.02	0.31	1.72	4.82	1.62	0.03	0.22	96.89
	stdev	1.14	0.04	0.76	0.14	0.02	0.24	0.37	0.23	0.11	0.03	0.06	2.53
Reclus	**R1**	***n = 107***											
	avg	76.87	0.12	13.06	1.20	0.04	0.21	1.47	4.11	2.68	0.03	0.20	96.14
	stdev	0.27	0.03	0.19	0.10	0.04	0.02	0.12	0.17	0.19	0.02	0.03	1.41
Lautaro/Viedma	**Historical**	***n = 36***											
	avg	75.30	0.30	13.34	1.57	0.03	0.27	1.87	3.72	3.37	0.06	0.17	97.34
	stdev	1.08	0.08	0.72	0.14	0.03	0.08	0.43	0.28	0.23	0.05	0.04	1.64

[a] Analyses determined using wavelength dispersive electron microprobe analysis.

3.1.1. Hudson

Hudson volcano has had four large eruptions since the LGM, producing widespread tephra deposits in the Patagonia-Tierra del Fuego region: H_0 at 17.38 ± 0.12 cal ka BP (Bendle et al., 2017; Weller et al., 2014), H_1 at ~7.75 ka cal BP, H_2 at ~3.92 ka cal BP and AD 1991 (Stern, 2008). In this study, analysis was undertaken on H_1 and H_2 tephra samples from different sites (Table 1).

Hudson tephra deposits are compositionally typified by a relatively low silica content (62–69 wt% SiO_2 for H_1 and H_2 deposits) in comparison to products erupted by AVZ centres (Section 3.1.2-3.1.4; Table 2; Fig. 3). The H_2 deposit has an average silica content of ~69.02 SiO_2 wt% and is thus a trachyrhyolite; the H_2 deposit is enriched in Na_2O, with an average content of ~5.88 wt% and it also has an average K_2O content of ~3.62 wt%. The H_1 deposit has an average silica content of ~63.72 wt% and is thus a trachydacite. The H_1 deposit has high contents of FeO, MgO and CaO, with averages of 4.81 wt%, 1.49 wt%, and 3.02 wt%, respectively. The average K_2O content of the H_1 deposit is ~2.83 wt% (Table 2).

3.1.2. Mt Burney

Mt Burney has had two volcanic eruptions that have emplaced widespread tephra across the Patagonia-Tierra del Fuego region: MB_1 and MB_2. The age of MB_1 is poorly constrained, with several different (but overlapping) dates in the literature, including 8.85–9.95 ka cal BP (Stern, 2008), 9.00–9.18 ka cal BP (Kilian et al., 2003) and 8.85–10.24 ka cal BP (Wastegård et al., 2013). MB_2 is deposited between 3.82 and 4.71 ka cal BP (Stern, 2008).

MB_1 and MB_2 are both rhyolitic and are chemically indistinct from one another, with combined averages of 76.17 wt% SiO_2; both layers are also potassium-poor, with combined averages of 1.67 wt% K_2O. The potassium content of Mt Burney deposits is a distinct feature as it is significantly lower than that of tephra from other AVZ centres (Sections 3.1.3, 3.1.4; Table 2; Fig. 3). In addition, Mt Burney deposits have higher sodium and magnesium contents than those of both Reclus and Lautaro/Viedma deposits with MB_1 deposits averaging 4.79 wt% Na_2O and 0.37 wt% MgO, and MB_2 deposits averaging 4.82 wt% Na_2O and 0.31 wt% MgO. As such these

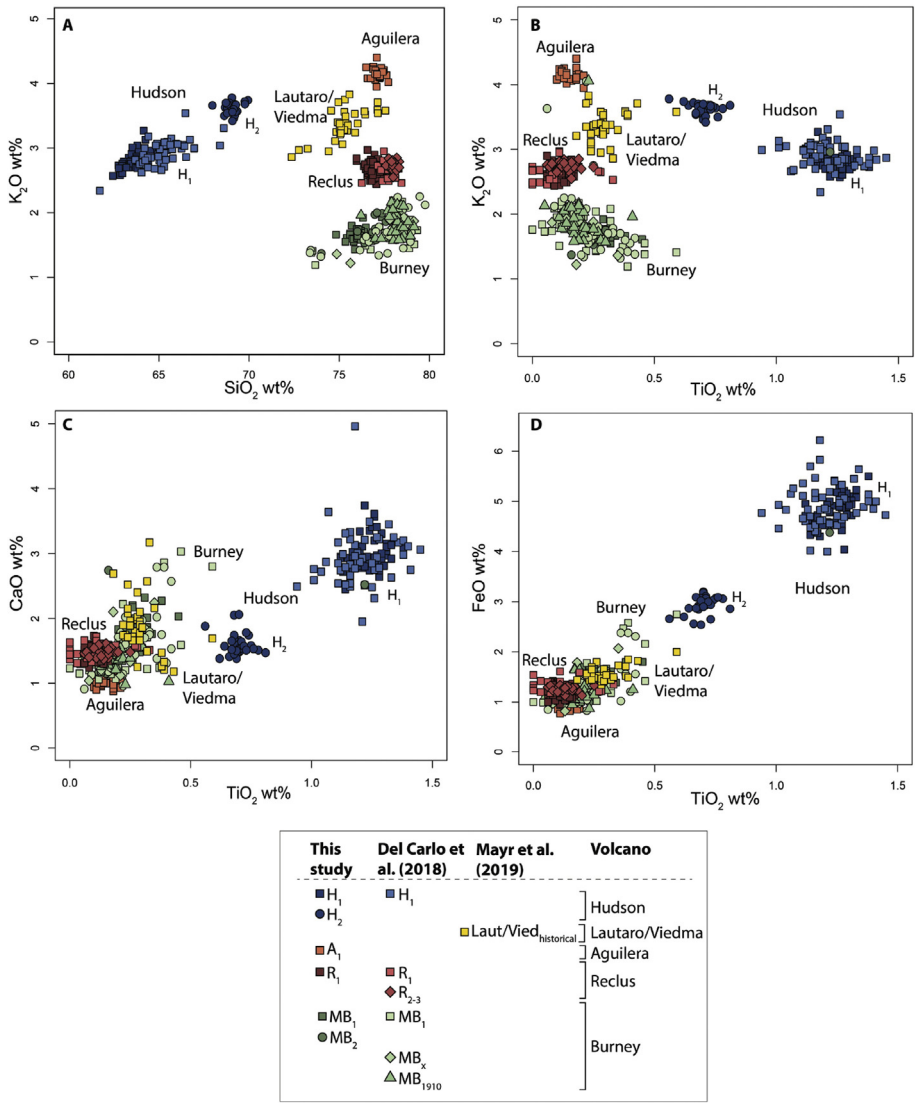

Fig. 3. Glass-shard geochemistry from regional marker horizons, including new data from this study, from Del Carlo et al. (2018) and from Mayr et al. (2019); see key for details.

chemicals are useful indicators to characterise the Mt Burney source.

3.1.3. Reclus

The main widespread deposit documented for Reclus is the rhyolitic R_1 tephra unit at 14.76 ± 0.18 ka cal BP (Stern et al., 2011). Two other tephra deposits with Reclus composition are identified in the Tierra del Fuego area (R_2 and R_3). These were deposited ~2.00 ka cal BP (Villa-Martínez and Moreno, 2007). Recent work by Del Carlo et al. (2018) have identified one of these units (i.e., R_2 or R_3) and provided a more precise age of <3.39–3.59 ka cal BP.

Deposits from Reclus are the most silica-enriched of all the deposits from AVZ centres; The SiO_2 content of R_1 deposits range between 75.96 and 77.79 wt%. The R_1 deposit contains on average 2.68 wt% K_2O (Table 2; Fig. 3), which distinguishes it from deposits of other centres, such as Lautaro/Viedma. However, since glass analyses are only available for widespread Reclus deposits: R_1 and $R_{2\text{-}3}$ (LA-1B in Del Carlo et al., 2018), it is possible that the compositional field is not representative of all deposits from Reclus volcano.

3.1.4. Lautaro/Viedma

This study incorporates chemical data published by Mayr et al. (2019) who describe the chemistry of seven historical rhyolitic tephra layers in lake sediment cores ~40–60 km southeast of the Lautaro volcano. Based on geography and dating, Lautaro volcano is the most likely source of six of these tephras, and Viedma volcano the source of one (Mayr et al., 2019). The chemistry of these deposits are similar, and in i) the absence of other known widespread tephra deposits from these volcanoes, and ii) the inability to differentiate between them, we use the compositions from Mayr et al. (2019) as a reference for Lautaro/Viedma chemistry. The chemistry of these deposits is similar to that of Reclus tephras, although Lautaro/Viedma deposits are more enriched in TiO_2 (~0.30 wt%) and K_2O (~3.37 wt%) than those from Reclus (~0.12 and ~2.68 wt%, respectively). There is only limited data from these two centres, and it is possible that other deposits may show greater compositional variability than what is shown in Fig. 3.

3.1.5. Aguilera

There was one large, widespread eruption from Aguilera volcano, called A_1, between 3.07 and 3.34 ka cal BP (Stern, 2008). Tephra deposits >10 cm thick and >5 cm thick have been identified

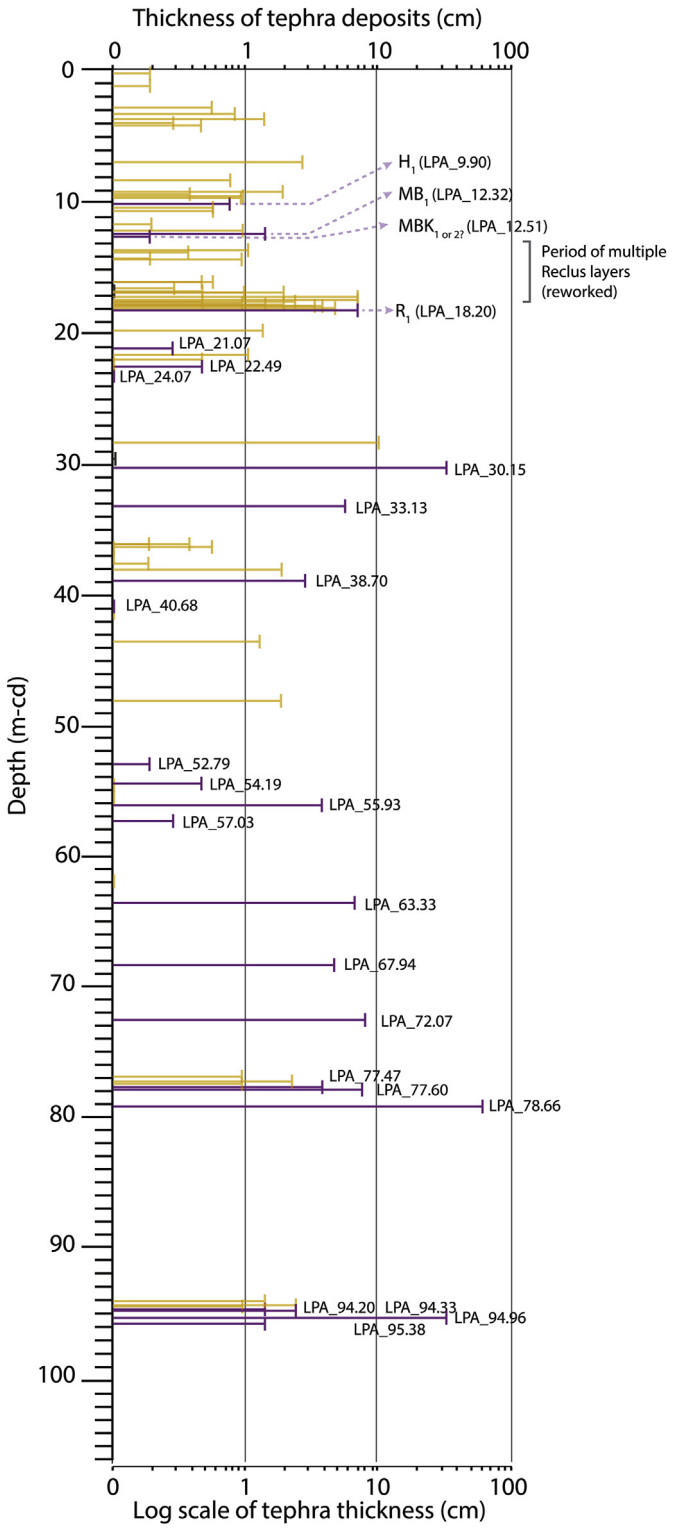

Fig. 4. Logarithmic scale of tephra thicknesses, with primary (purple) and reworked (orange) tephra layers. Tephra labels are provided for primary layers only. (For interpretation of the references to colour in this figure legend, the reader is referred to the Web version of this article.)

80 km and 130 km east from the centre, respectively. The identification of these thick A_1 tephra deposits indicates an eruption volume greater than MB_2 ($\geq$2.8 km^3) or the Hudson 1991 ($\geq$3.6 km^3) eruptions (Stern, 2008). Other smaller eruptions of Aguilera volcano have been reported in the Holocene but their deposits have been less widely dispersed and they have only been identified in Torres del Paine, Chile and Lago Argentino. (e.g., Stern, 2008; Strelin and Malagnino, 2000). Further work is required to refine the dates and chemical signatures of these.

Aguilera deposits are characterised by a high potassium content, which ranges from 3.95 to 4.40 wt%. The A_1 tephra also has a high average silica content of 77.12 wt%. In contrast to other widespread AVZ tephra deposits, A_1 deposits have low contents of Al_2O_3, FeOt and Na_2O, with averages of 12.62, 0.98 and 3.57 wt%, respectively. Sodium may be a useful tool for distinguishing tephra from NAVZ centres as it is particularly distinct when compared to the composition of other centres (Table 2), though caution should be taken since sodium is a mobile element that easily migrates with alteration.

3.2. Tephra units from Laguna Potrok Aike and their glass chemical composition

We identified 94 visible tephra deposits through the sedimentary sequence ranging in thickness from 0.1 to 35.5 cm (Fig. 4); these predominantly had sharp bases separated by pelagic sediment, were light in colour and fine-grained. Seventy-nine of these deposits were rhyolitic, one was rhyodacitic, and ten were trachydacitic; only four tephra layers could not be analysed due to low abundances of glass-shards (Fig. 4). Variations in the major element glass composition of the Laguna Potrok Aike tephra allows these tephra units to be assigned to four broad groups that correspond to different volcanic sources; tephra was assigned to a group based on its dominant chemical composition (described in Section 3; Fig. 5). These compositional groups can also be used to identify reworked deposits as they often have heterogeneous compositions that span multiple groups atypical of a primary ashfall event.

Based on tephra compositional and morphological information, 65 tephra deposits identified are considered to be reworked, three are potentially reworked, 25 are primary, and there is insufficient information for one tephra. Further detail on these deposits is provided in Section 4. Here the chemical compositions of both primary and reworked tephra are discussed.

3.2.1. Group 1 tephra

Group 1 includes nine tephra layers (LPA_0.12, 4.17, 6.89, 8.35, 9.26, 9.33, 9.52, 9.67, 9.90) that have been deposited between 0.08 and 8.4 ka cal BP. Tephra deposits belonging to this group are dark and medium grained (0.25–0.5 mm). Glass-shards forming tephra layers in this group are typically yellow or green in colour and have a vesicular or fluted morphology (Fig. 2). Their free-crystal mineral assemblage is composed of plagioclase, quartz, orthopyroxene and minor hornblende.

The chemical composition of four deposits in Group 1 is heterogeneous and the group is subsequently sub-divided into A- and B-type tephra with B-type tephra reflecting heterogeneous compositions. Group 1A tephra can be identified by their trachydacitic affinities, with intermediate SiO_2 content (~64.22 wt%) and intermediate-high K_2O content (~2.84 wt%). Group 1A tephra has a high Al_2O_3 content, ranging from 15.50 to 18.06 wt%, and a high Na_2O content, ranging from 5.21 to 6.51 wt%.

3.2.2. Group 2 tephra

Group 2 tephra consists of 19 layers that occur between 12.32 m-cd and 95.39 m-cd (9.42–50.86 ka cal BP; LPA_12.32, 12.51, 21.42, 21.98, 28.23, 30.15, 38.04, 38.70, 40.68, 54.19, 57.03, 67.94, 72.07, 93.99, 94.09, 92.20, 94.33, 94.96, and 95.38). The deposits included in this group comprise colourless shards that have a fluted and vesicular morphology; the vesicle shape varies between

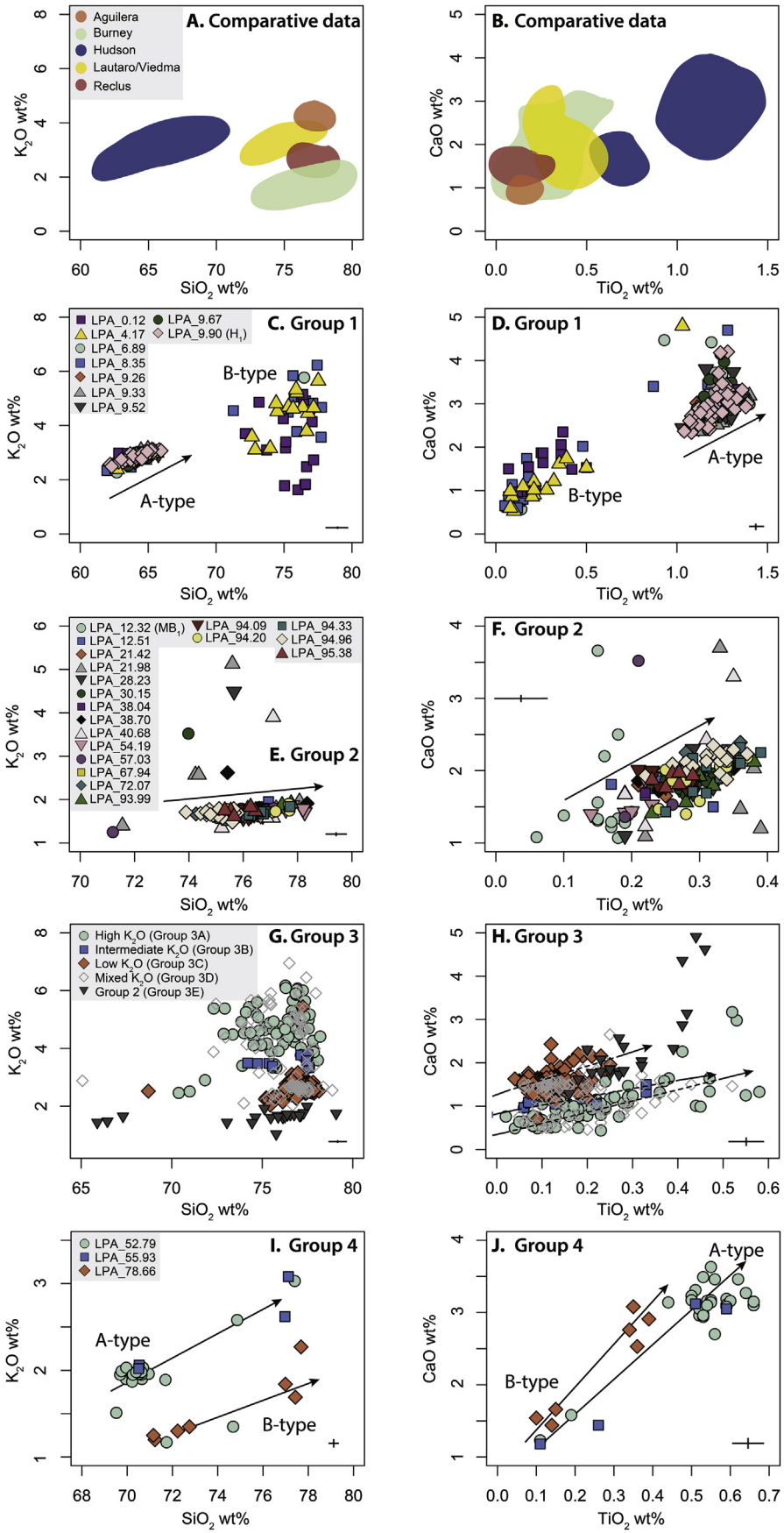

Fig. 5. Variation diagrams of glass-chemical data for tephra identified in the Laguna Potrok Aike sedimentary sequence. Compositional trends are identified using black arrows. A-B) Compositional fields of widespread marker horizons extracted from the terrestrial realm (this study; Del Carlo et al., 2018); C-D) Group 1 tephra. Some of these deposits have two components (Group 1A from Hudson volcano and Group 1B from AVZ sources; see Section 4); E-F) Group 2 tephra (from Mt Burney); G-H) Group 3 tephra (from Reclus volcano and AVZ centres); I-J) Group 4 tephra (from unknown centres). Error bars represent 2 standard deviations of repeated analyses of the StHs6/80-G MPI-DING reference glass. Note that axes are different in scale for each figure.

circular and elongate. There are additionally white-grey pumice particles rich in dark micro-phenocryst inclusions in these deposits. Group 2 deposits are typically characterised by ~50% glass-shards and a high abundance of minerals (~40%). The mineral assemblage of Group 2 deposits is composed of plagioclase, orthopyroxene, olivine and hornblende with some tephra samples also having quartz.

The glass-chemical composition of Group 2 tephra is rhyolitic with low potassium (~1.79 K_2O wt%) and intermediate-high magnesium contents (~0.37 MgO wt%; Table 3; Fig. 5). Group 2 tephra deposits have intermediate FeO_t contents, typically between 0.95 and 2.39 wt%, intermediate TiO_2 contents, typically between 0.06 and 0.39 wt%, and high Na_2O contents, typically between 2.43 and 5.19 wt%.

3.2.3. Group 3 tephra

Group 3 tephra consists of 47 tephra layers, which occur between 1.75 m-cd and 77.69 m-cd (1.3–63.1 ka cal BP) and are the most commonly identified tephra type (Table 3; Fig. 5). Group 3 tephra predominantly consist of colourless glass-shards with cuspate and fluted shard morphology. On occasion, grey pumice with microlite inclusions, as well as platy, colourless shards are also present. Tephra from this group usually have a mineral assemblage consisting of plagioclase, orthopyroxene, and occasionally olivine and hornblende. Very low abundances of biotite are observed in LPA_1.08, 2.56, and 63.33.

Group 3 tephra deposits are rhyolitic in composition and have quite variable potassium contents (~3.22 K_2O wt%; range: 1.04–6.95 K_2O wt%). Based on potassium content, Group 3 tephra are sub-classified into five groups: 3A) high, 3B) intermediate, 3C) low, 3D) mixed, and 3E) very low abundance potassium (in respect to the abundance of potassium identifiable in Group 3 tephra deposits). Group 3A, 3B and 3C have average K_2O contents of 4.64 wt% ($n = 75$), 3.40 wt% ($n = 16$), and 2.66 wt% ($n = 475$), respectively. Group 3D shows a range between 2.04 and 6.95 wt% K_2O ($n = 111$). There are some chemical outliers (Group 3E) amongst Group 3 tephra that are more comparable to Group 2 tephra compositions. Because of this, they are listed as Group 2 (Group 3E) chemistry in Fig. 5 – these have a very low average potassium content of 1.63 wt % K_2O (range: 1.04–1.99 wt%; $n = 27$).

The tephra layers in Group 3A are LPA_35.97, 36.04, 36.15, 42.00, 55.40, and 61.67; Group 3B layers are LPA_12.16 and 63.33; Group 3C layers are LPA_10.49, 10.59, 11.71, 16.11, 16.48, 16.78, 16.91, 16.92, 16.97, 17.19, 17.39, 17.55, 17.59, 17.62, 17.64, 17.65, 17.69, 17.75, 17.76, 17.79, 17.80, 17.85, 17.90, 18.03, 18.20, 77.04, 77.47, 77.61, and Group 3D layers are LPA_1.08, 13.62, 14.20. Group 3D/3E layers are, LPA_21.07, 2.56, 24.07, 37.55; Group 3C/3E layers are, LPA_14.22, 16.04, Group 3A/3E layers are, LPA_36.80, 43.46; Supplementary File 2).

Titanium and calcium are useful to further differentiate the different sub-classifications of Group 3 tephra. Tephra in Group 3A have a low abundance of CaO (~1.01 wt%) and a relatively narrow range of TiO_2 (0.02–0.58 wt%). This contrasts with Group 3C, which has a higher abundance of CaO (~1.55 wt%) and a low abundance of TiO_2, with a mean of ~0.13 wt% and wider range of 0.04–0.91 wt%. The sample size of Group 3B is quite limited ($n = 11$), but tephra in this group have similar calcium and titanium contents compared to those in Group 3A.

3.2.4. Group 4 tephra

Group 4 consists of 3 tephra layers observed at 52.79 m-cd (~40.8 ka cal BP), 55.93 m-cd (~44.6 ka cal BP), and 78.66 m-cd (~64.7 ka cal BP), respectively. Group 4 can be subdivided into two groups: 4A and 4B. Group 4A has, on average, slightly higher K_2O content than 4B (71.35 and 74.21 wt%, respectively).

Group 4A includes LPA_52.79 and LPA_55.93. LPA_52.79 is a 0.2 cm thick unit of grey/white pumice with dark microphenocryst inclusions and spherical vesicles. The mineral content is <10% and comprises plagioclase, orthopyroxene, biotite, olivine and quartz. Accidental lithics are abundant in this sample at ~25%. Chemically, it has an intermediate potassium content with respect to its silica content (~2.46 wt% K_2O and 70.99 wt% SiO_2). This chemical signature is not observed in any other group. TiO_2 (~0.53 wt%) and Al_2O_3 (~15.10 wt%) are relatively abundant. LPA_52.79 tephra chemistry follows similar K_2O/SiO_2 evolutionary trends to Group 3B tephra, but has different CaO/TiO_2 compositions (Table 3; Fig. 5). LPA_55.93 is a 4 cm unit of white and colourless, crystal-poor, (spherical) vesicular and fluted shards. Glass-shard abundance is 85%, while lithics and minerals comprise 15% of the sample. Bottle-green orthopyroxene with Fe-Ti oxides, plagioclase, and hornblende form the mineral assemblage of this deposit. Chemically, LPA_55.93 is a rhyolite with a heterogeneous composition. The deposit has a SiO_2 range from 70.51 to 77.12 wt%.

Group 4B consists only of LPA_78.66, which is a ~63 cm thick cream-coloured unit that comprises white microphenocryst-poor pumice, and a minor abundance of vesicular and fluted colourless glass-shards. Overall, this unusually thick deposit is crystal-poor (<5%), with only green orthopyroxene with Fe-Ti oxide inclusions and plagioclase. LPA_78.66 is chemically heterogeneous, with a SiO_2 content between 71.16 and 77.68 wt%, and a K_2O content between 1.70 and 2.77 wt%.

4. Interpretation and discussion

4.1. Chemical fingerprints and tephra correlations

In this section, tephra is correlated to source centres in the lowermost SVZ and AVZ on the basis of tephra chemistry. Tephra has been correlated to Hudson volcano, Mt. Burney, Reclus and NAVZ centres.

4.1.1. Hudson volcano

Group 1A tephra deposits (Fig. 5C–D; Section 3.2.1) can be correlated with volcanism from Hudson volcano based on glass-shard geochemistry, and notably their intermediate silica content and intermediate-high potassium content (Figs. 5C–D, 6; Section 3.2.1). Hudson volcano is located approximately 700 km from Laguna Potrok Aike. The widespread H_1 deposit from Hudson volcano was previously identified in the Laguna Potrok Aike record obtained for the SALSA campaign (Haberzettl et al., 2007, Section 2.2). However, this chemically distinct tephra layer was never identified in the Laguna Potrok Aike record obtained for the PASADO campaign (Kliem et al., 2013a; Wastegård et al., 2013). The H_1 (LPA_9.90) deposit has now been identified as a coarse, 9.6 cm thick ash between 9.90 and 10.00 m-cd in the sediment sequence, and has a depositional age of 8.6–9.0 ka cal BP (Table 4; Fig. 6). The age for this tephra from the Laguna Potrok Aike age model is somewhat older than most previously published ages for H_1 (Stern, 1992, 2008; Prieto et al., 2013; Naranjo and Stern, 1998) but does overlap with reported ages of 8.42–8.63 ka cal BP for this tephra from lake cores near Cochran, Chile, 150 km southeast of the volcano (Stern et al., 2016).

After the deposition of this primary unit (stratigraphically upcore), there are five tephra layers with a Hudson affinity which are reworked, and two which are likely reworked (Figs. 4 and 9; Supplementary File 2). These are identified by a dominance of rounded and sub-rounded minerals (Fig. 2), a lack of glass coating on minerals (particularly on orthopyroxene), a decline in the overall abundance of glass-shards, an increase in the abundance of lithics, and in some cases, an increase in the abundance of organic

Table 3
Average and standard deviation of glass-shard chemistry for the different groups of tephra identified in the Laguna Potrok Aike sequence, including Groups 1 (A and B-type), 2, 3 (3A, 3B, 3C, 3D, 3E) and 4 (4A and 4B) (total $n = 1046$). This data includes reworked and primary tephra chemistry. Tephra chemistry is normalised to 100 wt%. Total represents analytical total. Dataset presented in Supplementary File 1.

Group		SiO_2	TiO_2	Al_2O_3	FeOt	MnO	MgO	CaO	Na_2O	K_2O	P_2O_5	Cl	Total
Group 1	A-type	***n = 182***											
	average	64.22	1.22	15.94	4.8	0.16	1.45	3.03	5.85	2.84	0.36	0.14	98.81
	stdev	0.77	0.08	0.3	0.32	0.05	0.23	0.42	0.25	0.15	0.05	0.03	1.25
	B-type	***n = 41***											
	average	75.65	0.21	13.02	1.58	0.06	0.2	1.22	3.71	4.12	0.04	0.19	96.06
	stdev	1.58	0.13	0.65	0.5	0.04	0.15	0.47	0.61	1.15	0.04	0.04	1.83
Group 2		***n = 150***											
	average	76.09	0.28	13.14	1.53	0.05	0.37	1.9	4.59	1.79	0.05	0.22	95.92
	stdev	1.09	0.06	0.56	0.24	0.04	0.08	0.41	0.33	0.46	0.03	0.04	1.8
Group 3	Group 3A	***n = 77***											
	average	75.79	0.21	12.91	1.42	0.07	0.17	1.01	3.54	4.65	0.03	0.2	95.39
	stdev	1.63	0.13	0.63	0.56	0.04	0.13	0.47	0.52	0.81	0.03	0.05	1.11
	Group 3B	***n = 11***											
	average	76.4	0.16	13.06	1.31	0.06	0.16	1.24	4.1	3.35	0.03	0.13	95.08
	stdev	1.21	0.1	0.22	0.59	0.03	0.06	0.21	0.28	0.37	0.02	0.08	1.23
	Group 3C	***n = 475***											
	average	77.15	0.13	12.96	1.23	0.05	0.22	1.55	3.82	2.66	0.03	0.22	96.27
	stdev	0.57	0.05	0.23	0.20	0.04	0.04	0.14	0.30	0.17	0.02	0.09	2.69
	Group 3D	***n = 101***											
	average	78.87	0.18	12.94	1.37	0.05	0.2	1.25	3.75	3.8	0.04	0.19	96.1
	stdev	65.07	0.13	0.59	0.49	0.04	0.14	0.44	0.61	1.27	0.04	0.04	1.76
	Group 3E	***n = 23***											
	average	74.93	0.29	13.69	1.85	0.05	0.52	2.37	4.39	1.64	0.06	0.2	97.17
	stdev	3.54	0.09	1.36	0.8	0.03	0.46	0.99	0.58	0.19	0.06	0.06	1.69
Group 4	Group 4A	***n = 31***											
	average	71.35	0.51	14.93	2.51	0.05	0.74	2.93	4.18	2.52	0.12	0.18	96.61
	stdev	2.27	0.14	0.87	0.58	0.04	0.22	0.64	0.40	0.38	0.05	0.03	1.94
	Group 4B	***n = 7***											
	average	70.12	0.45	14.43	2.39	0.05	0.67	2.75	4.10	2.39	0.11	0.17	94.15
	stdev	3.01	0.12	1.13	0.74	0.06	0.21	0.70	0.44	0.40	0.55	0.02	1.54

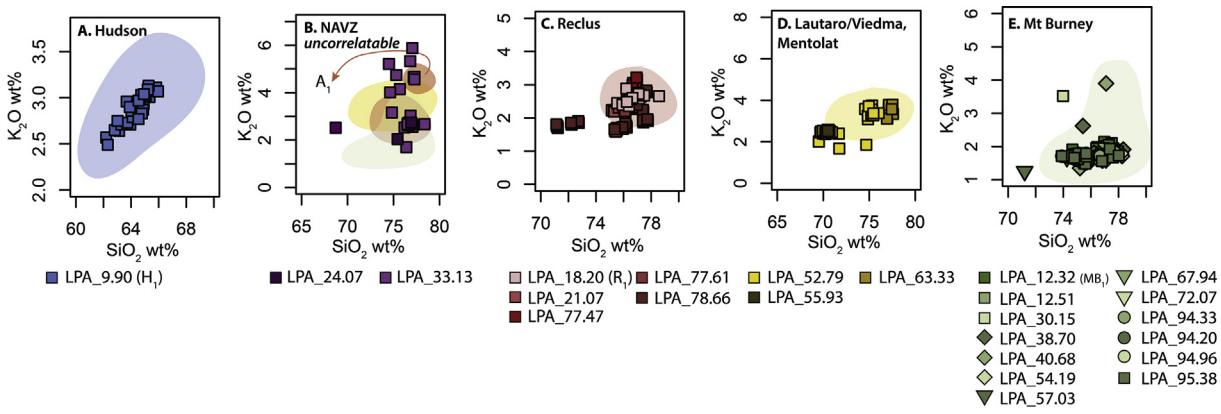

Fig. 6. Variation diagrams of glass-chemical data for tephra deposited via primary ash-fall at individual centres identified in the Laguna Potrok Aike sedimentary sequence: A) Hudson; B) uncorrelatable deposits from the NAVZ; C) Reclus; D) Lautaro/Viedma or Mentolat; E) Mt Burney. Compositional fields of widespread marker horizons are extracted from the terrestrial realm (this study; Del Carlo et al., 2018; Mayr et al., 2019) and are represented using the same colours as for Fig. 3 and 5. (For interpretation of the references to colour in this figure legend, the reader is referred to the Web version of this article.)

material. Sedimentation rates vary during this period (e.g., Kliem et al., 2013a) and it is considered likely that the redeposition of tephra during the last ~8 ka cal BP is related to lake level changes that caused reworking of older sediments (Anselmetti et al., 2009; Haberzettl et al., 2007; Kliem et al., 2013b; Zolitschka et al., 2013, Section 4.3).

The analysis of individual deposits indicates that LPA_9.90 is the only primary tephra unit with a Hudson affinity in the Laguna Potrok Aike sedimentary record. Much of the up-core reworking shares the same tephra chemistry as the LPA_9.90 unit. However, there are four deposits with a larger compositional range (LPA_0.12, 4.17, 6.89, and 8.35). The Group 1 A-type composition of these deposits has Hudson affinity, but the occurrence of Group 1 B-type glass is more consistent with AVZ volcanism (Fig. 5A–B; Sections 3.2.1, 4.3). The heterogeneity in this glass chemistry is deemed to be further evidence of reworking.

The widespread and compositionally unique H_2 marker horizon, deposited ~3.92 ka cal yr BP (Naranjo and Stern, 1998), has not been identified in the Laguna Potrok Aike sedimentary record indicating limited possibility of other Hudson volcano sources for reworking than the LPA_9.90, H_1 unit.

4.1.2. Mt Burney

Group 2 tephra deposits (Fig. 5E–F; Section 3.2.2) are associated

Table 4
Average and standard deviation of glass-shard chemistry for the primary tephra layers identified in the Laguna Potrok Aike sedimentary sequence (this study; Supplementary Files 1, 2). Tephra chemistry is normalised to 100% and analytical total is presented.

Tephra label and correlation		SiO_2	TiO_2	Al_2O_3	FeOt	MnO	MgO	CaO	Na_2O	K_2O	P_2O_5	Cl	Total
Hudson - H1													
LPA_9.90	avg	64.36	1.21	15.91	4.79	0.16	1.46	2.98	5.75	2.89	0.36	0.13	98.88
n = 43	stdev	0.84	0.09	0.12	0.30	0.06	0.27	0.42	0.23	0.15	0.05	0.02	0.99
Mt. Burney - MB1													
LPA_12.32	avg	77.11	0.16	12.86	1.08	0.04	0.26	1.56	4.68	1.97	0.04	0.23	95.49
n = 17	stdev	0.75	0.03	0.19	0.10	0.03	0.02	0.65	0.15	0.08	0.03	0.02	2.28
Mt. Burney - MBK1/2?													
LPA_12.51	avg	76.36	0.26	13.12	1.52	0.04	0.35	1.84	4.55	1.68	0.04	0.24	97.63
n = 12	stdev	0.54	0.05	0.26	0.15	0.04	0.04	0.17	0.14	0.11	0.03	0.02	1.98
Reclus - R1													
LPA_18.20	avg	76.76	0.17	12.92	1.35	0.04	0.26	1.69	4.02	2.57	0.04	0.18	95.70
n = 18	stdev	0.67	0.05	0.39	0.20	0.04	0.08	0.18	0.23	0.13	0.03	0.03	1.62
Reclus													
LPA_21.07	avg	75.58	0.22	13.52	1.67	0.06	0.32	2.10	4.15	2.19	0.04	0.14	98.34
n = 7	stdev	0.28	0.05	0.22	0.09	0.05	0.05	0.09	0.26	0.26	0.02	0.03	2.50
Insufficient chemistry													
LPA_22.49													
NAVZ - Unknown													
LPA_24.07	avg	76.56	0.13	13.08	1.28	0.06	0.18	1.27	3.86	3.34	0.03	0.21	96.58
n = 28	stdev	0.86	0.06	0.32	0.38	0.04	0.06	0.37	0.50	1.09	0.03	0.03	1.75
Mt. Burney													
LPA_30.15	avg	76.13	0.28	12.97	1.57	0.03	0.38	1.85	4.62	1.87	0.04	0.24	95.59
n = 12	stdev	0.79	0.04	0.25	0.28	0.04	0.04	0.10	0.31	0.52	0.02	0.04	1.07
NAVZ - Unknown													
LPA_33.13	avg	73.69	0.40	13.63	2.61	0.04	0.49	2.05	4.37	2.43	0.12	0.18	96.89
n = 3	stdev	4.38	0.45	0.64	1.90	0.07	0.31	0.51	0.44	0.36	0.13	0.01	1.82
Mt. Burney													
LPA_38.70	avg	76.47	0.26	13.20	1.46	0.08	0.33	1.83	4.15	1.96	0.05	0.23	95.27
n = 5	stdev	1.14	0.05	0.41	0.10	0.06	0.03	0.13	0.97	0.38	0.02	0.05	1.61
Mt. Burney													
LPA_40.68	avg	76.32	0.26	13.24	1.40	0.02	0.31	2.02	4.36	1.83	0.06	0.18	96.48
n = 10	stdev	0.73	0.05	0.42	0.18	0.03	0.08	0.55	0.53	0.73	0.02	0.03	1.15
NAVZ - Lautaro/Viedma or Mentolat													
LPA_52.79	avg	70.99	0.53	15.10	2.59	0.05	0.77	3.03	4.18	2.46	0.13	0.18	96.97
n = 27	stdev	1.80	0.12	0.63	0.47	0.04	0.18	0.51	0.42	0.33	0.04	0.03	1.63
Mt. Burney													
LPA_54.19	avg	77.39	0.21	12.91	1.23	0.04	0.29	1.59	4.42	1.74	0.04	0.14	94.73
n = 6	stdev	0.95	0.05	0.43	0.19	0.04	0.04	0.22	0.20	0.09	0.02	0.03	1.16
NAVZ - Lautaro/Viedma or Mentolat													
LPA_55.93	avg	73.78	0.37	13.79	1.97	0.03	0.49	2.20	4.17	2.94	0.07	0.18	94.84
n = 4	stdev	3.77	0.22	1.45	1.00	0.02	0.32	1.03	0.25	0.50	0.06	0.04	2.44
Mt. Burney													
LPA_57.03	avg	75.36	0.22	14.20	1.15	0.05	0.28	2.14	4.76	1.64	0.07	0.14	94.51
n = 3	stdev	3.62	0.03	2.40	0.06	0.08	0.02	1.20	0.27	0.34	0.02	0.02	0.77
Lautaro/Viedma													
LPA_63.33	avg	77.32	0.09	13.04	0.81	0.04	0.11	1.09	3.91	3.51	0.01	0.06	94.90
n = 5	stdev	0.28	0.03	0.23	0.12	0.02	0.04	0.09	0.08	0.29	0.01	0.02	0.55
Mt. Burney													
LPA_67.94		75.68	0.33	13.02	1.86	0.07	0.43	2.00	4.67	1.64	0.06	0.24	96.04
n = 1													
Mt. Burney													
LPA_72.07	avg	74.71	0.32	13.65	1.88	0.04	0.53	2.32	4.64	1.64	0.06	0.21	97.37
n = 2	stdev	0.64	0.05	0.05	0.05	0.01	0.09	0.09	0.23	0.05	0.02	0.01	0.59
Reclus													
LPA_77.47	avg	76.72	0.10	13.22	1.22	0.04	0.20	1.29	4.06	2.95	0.04	0.16	94.22
n = 5	stdev	0.29	0.02	0.07	0.27	0.03	0.02	0.14	0.14	0.19	0.02	0.02	0.70
Reclus													
LPA_77.61	avg	76.78	0.14	13.21	1.26	0.08	0.23	1.59	4.02	2.48	0.03	0.18	94.32
n = 5	stdev	0.41	0.01	0.07	0.22	0.06	0.07	0.17	0.13	0.25	0.03	0.01	0.61
Reclus													
LPA_78.66	avg	74.21	0.26	14.08	2.11	0.07	0.44	2.27	4.27	2.06	0.08	0.15	96.06
n = 7	stdev	3.01	0.12	1.13	0.74	0.06	0.21	0.70	0.44	0.40	0.05	0.02	1.54
Mt. Burney													
LPA_94.20	avg	76.23	0.30	12.91	1.59	0.06	0.40	1.92	4.62	1.69	0.05	0.22	96.39
n = 13	stdev	0.91	0.04	0.46	0.23	0.05	0.05	0.28	0.18	0.09	0.02	0.03	1.39
Mt. Burney													
LPA_94.33	avg	75.96	0.33	12.99	1.66	0.05	0.43	2.05	4.61	1.65	0.04	0.22	96.45
n = 15	stdev	0.75	0.04	0.35	0.12	0.05	0.05	0.26	0.16	0.08	0.02	0.02	1.35
Mt. Burney													
LPA_94.96	avg	75.02	0.31	13.53	1.73	0.05	0.46	2.13	4.80	1.67	0.06	0.24	95.48
n = 18	stdev	0.51	0.04	0.20	0.14	0.04	0.04	0.13	0.18	0.08	0.02	0.01	1.45
Mt. Burney													
LPA_95.38	avg	75.95	0.26	13.37	1.48	0.04	0.37	1.88	4.63	1.73	0.05	0.23	95.42
n = 6	stdev	0.50	0.02	0.23	0.16	0.03	0.04	0.09	0.10	0.07	0.04	0.04	0.90

with Mt Burney volcanism. There is little chemical variation between the Mt Burney proximal data and the layers that have been correlated to Mt Burney volcano in the Laguna Potrok Aike sedimentary sequence. Of the 19 layers identified, 13 are primary and six are reworked deposits (Table 4; Figs. 6 and 7). This indicates that Mt Burney is possibly the most active volcanic centre in the AVZ through the Late Quaternary (Section 4.2).

The most widespread unit, MB_1 (LPA_12.32), is additionally identified in the PASADO sequence as a 1.5 cm thick deposit between 12.32 and 12.34 m-cd, which corresponds to an age of 10.0–10.4 cal ka BP. This age is slightly older than that of Stern (2008) and Kilian et al. (2003) who report a depositional age for this widespread eruption of 8.9–9.5 cal ka BP and 9.0–9.6 cal ka BP, respectively. However, it overlaps with that of Del Carlo et al. (2018) who report ^{14}C ages of between 9299 ± 65 and 7325 ± 46 ^{14}C yr BP (10.64 ± 0.10 and 8.10 ± 0.06 cal ka BP).

Some studies (e.g., Kilian et al., 2003; Monteath et al., 2019; Stern, 2008) have reported Mt Burney-type tephra in the mid-Holocene. However, the largest of these, MB_2, is distributed well to the south, and we have not encountered any tephra layers after the deposition (up-core) of MB_1 in Laguna Potrok Aike with Mt Burney affinity. It is possible that Mt Burney tephra may be present as cryptotephra horizons (i.e., tephra not visible to the naked eye) rather than as visible tephra horizons. Cryptotephra was not analysed in this study because of the large number of visible and reworked tephra layers observed, which would result in a high background cryptotephra signal.

4.1.3. Reclus and NAVZ centres

The correlation of deposits to Reclus and individual NAVZ centres (Lautaro, Viedma, Aguilera) using major element glass compositions is difficult because they are compositionally similar to each other (e.g., Wastegård et al., 2013). While this study, in combination with Del Carlo et al. (2018), presents the most comprehensive glass-chemical dataset for proximal deposits in the southernmost part of South America, the dataset is still limited (Table 2; Fig. 3). It has been suggested that trace elements should be used to further differentiate these (Del Carlo et al., 2018; Wastegård et al., 2013). However, glass-shards in NAVZ deposits are typically very small (~10–15 μm) and their trace elemental chemical characterisation is very challenging due to technical limitations of LA-ICP-MS (e.g., beam size; Pearce, 2014; Tomlinson et al., 2010). Future work should involve expanding this reference dataset because the compositional fields may be larger than shown at present, and they may overlap with one other as only the widespread eruptive deposits have been characterised. Correlations made to individual centres in the NAVZ should therefore be treated with caution, and suggested source volcanoes are simply the most likely event source based on our current knowledge of the chemical composition at each.

Group 3 tephra (Table 3; Fig. 5G–H; Section 3.2.3) are representative of Reclus and NAVZ tephra. Aguilera, Lautaro and Reclus volcanoes can be sub-classified based on potassium, calcium and titanium contents (Table 4; Fig. 5), and these are likely to correspond to the following sources: 3A-Aguilera (high K_2O), 3B-Lautaro (intermediate K_2O), 3C-Reclus (low K_2O), 3D-reworked (mixed K_2O), and 3E-outliers (very low K_2O) from Groups 3A-D that correspond best with Group 2 (Mt Burney) chemistry (Table 3; Figs. 5G–H, 6; Supplementary File 2). The component of Group 1 labelled Type B is additionally most reflective of Group 3 tephra from the AVZ. These deposits have a very low average potassium content of 1.63 wt% K_2O (range: 1.04–1.99 wt%; $n = 27$). Moreover, tephra layer LPA_78.66, of Group 4B is tentatively correlated to Reclus volcano (low K_2O; Group 3C; Fig. 4G–H; Fig. 6) because, while it does not plot on the known compositional field of Reclus, it lies on the same compositional trend as other deposits from the centre. In addition, the chemistry of deposits in Group 4A correlate well with Lautaro/Viedma, or possibly Mentolat (Weller et al., 2019).

Some analyses in Group 3 (Fig. 5G–H) are heterogeneous, and possess a mixed potassium content (Group 3D), while some analyses are outliers from Groups 3A-3D but possess the same trend and composition of Group 2 (Mt Burney) and thus are sub-categorised (Group 3E). Many of these layers are reworked based on analysis of their mineral assemblage and glass-shards, in addition to heterogeneous chemical composition which is atypical of AVZ tephra deposits. Of Group 3 deposits, six are primary, 38 are reworked, and one is likely reworked; reworked deposits are discussed in detail in Section 4.3 (Supplementary File 2).

The sequence between 16.47 and 18.25 m-cd (~14.3 cal ka BP; Fig. 5) is composed of multiple thick and persistently light beige, fine-grained tephra with little pelagic sediment in between. In Kliem et al. (2013a), the R_1 tephra was placed at the top of this sequence, at 16.78–16.79 m-cd (0.5 cm thickness). The tephra beneath were overlooked because they were considered as being part of a prolonged period of sedimentary reworking (e.g., Kliem et al., 2013a). However, no primary tephra deposit was identified which leaves no mechanistic explanation for the presence of subsequent (upper-core) tephra layers. In other words, reworked layers (particularly thick ones) are very unlikely to exist without the deposition of an initial primary tephra layer, and this is (often) thicker than any subsequent reworked layers. We therefore suggest the bottom tephra in this sequence at 18.20–18.25 m-cd (14.1–14.5 cal ka BP) to be the primary R_1, with the subsequent sequence representing its reworked facies (Fig. 7).

Reclus volcano, located ~250 km northwest of Laguna Potrok Aike, deposited the large R_1 tephra horizon at 14.76 (±0.18) cal ka BP (date after Stern et al., 2011). Stern (2008) identified R_1 deposits in the terrestrial realm >10 cm thick, and >5 cm thick at 150 km and 350 km southeast of the volcano, respectively. The maximum observed thickness of R_1 was >40 cm, observed 90 km southeast from the volcano. Because the tephra thicknesses in lake environments are less affected by preservation issues than in their terrestrial counterparts (e.g., Fontijn et al., 2014) and the deposit had a south-south east dispersal, it is expected that the primary thickness of the R_1 deposit observed in Laguna Potrok Aike should be between 5 and 10 cm thick. As such, it is unlikely that the entire tephra-bearing sequence between 16.47 and 18.25 m-cd would correspond to R_1.

The visual and chemical analysis of numerous tephra layers in the sedimentary record between 16.47 and 18.25 m-cd, indicates that the initial 5-cm-thick, diffuse, beige, Group 3C tephra layer deposited at 18.20–18.25 m-cd (~14.3 cal ka BP) most likely corresponds to the large and widespread R_1 tephra layer. Subsequent tephra above this (including the tephra labelled as R_1 by Kliem et al., 2013a and Wastegård et al., 2013) with the same glass composition are most likely reworked. The deposition of the 5-cm-thick R_1 tephra on unconsolidated sediment on relatively steep slopes near the edge of the lake could have caused the sediment to destabilise, and resulted in multiple reworked tephra layers with sediment in-between (see Section 4.3; Fig. 7).

One tephra layer, LPA_63.33 (Group 3B; 43.4 cal ka BP) has a possible Lautaro/Viedma affinity based on comparisons to glass chemistry of proximal deposits from historical eruptions (Mayr et al., 2019). This possibly represents the first documentation of prehistoric Lautaro activity. Two tephra layers, LPA_52.79 and 55.93 (Group 4A; 34.2 and 35.6 cal ka BP, respectively) are also chemically similar to Lautaro/Viedma. However, these deposits of rhyolitic and rhyodacitic composition have a slightly lower silica and potassium abundance than the known Lautaro/Viedma compositional field for

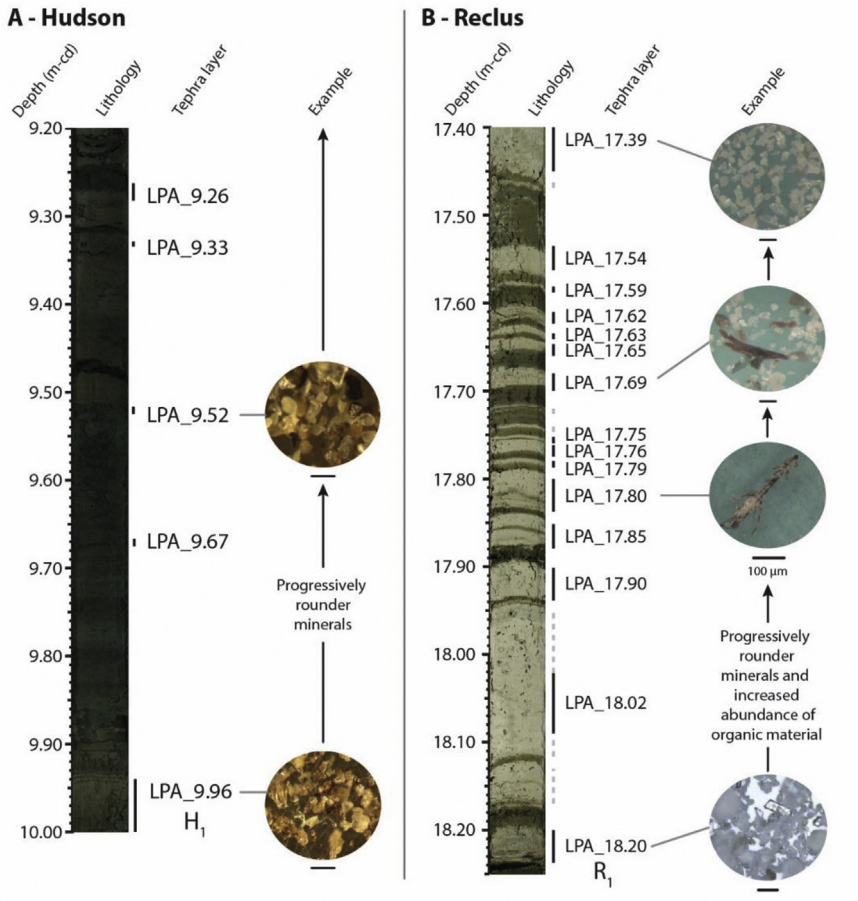

Fig. 7. Illustration of reworked tephra deposits in the Laguna Potrok Aike sedimentary sequence. In both of these instances, an initial widespread tephra marker is succeeded by periods of pelagic sedimentation and further tephra layers. All tephra layers that are identified after the initial event have the same chemical composition as the first deposit, and analyses of the deposits indicate that these are reworked – notably by the increased appearance of rounded minerals, decreased abundance of glass-shards, and increased abundance of organic material. A) shows the H_1 (Hudson) event, and subsequent (up-core) identified tephra layers, all with Hudson compositions; B) shows the R_1 (Reclus) event, and subsequent (up-core) identified tephra layers, all with Reclus compositions. There are clear implications for the assumption that discrete visible tephra layers, or cryptotephra layers with a substantial amount of pelagic sediment between events, are the product of primary fallout. It is important to note that the sharp tephra boundaries observed in B) of the composite record are not seen in all core-sections.

historical events (Section 3.1.4, Figs. 3, 5 and 6). The presence of olivine in LPA_52.79, lack of biotite in LPA_55.93, and the presence of accidental lithic clasts in both, typical of products associated with Mentolat volcanism (Weller et al., 2019), suggests that both layers could also possibly derive from eruptions of this volcano. We therefore tentatively attribute LPA_52.79 and LPA_55.93 to eruptions of either Lautaro/Viedma or Mentolat affinity, and require more proximal glass-shard chemical data from these centres to confirm their source.

Fifty-one deposits have a possible Reclus and/or NAVZ affinity (Group 3 and 4; Fig. 4E–J; Supplementary File 2). Most of these layers are reworked (41 = reworked; 9 = primary; 1 = likely reworked; Section 4.3). Of the nine primary tephra layers, one cannot be correlated to its source in the NAVZ (LPA_24.07), one is possibly correlated to Lautaro/Viedma (LPA_63.33), two are possibly correlated to Lautaro/Viedma or Mentolat (LPA_52.79 55.93), and five are correlated to Reclus (LPA_18.20 (=R_1), 21.07, 77.47, 77.61, 78.66). LPA_24.07 was deposited at 18.1 cal ka BP, and the potassium content has a large range of between 1.70 and 5.88 wt%, indicating that it could be from any centre in the NAVZ. LPA_33.13 is additionally considered to be a primary tephra; this unit has scarce chemical data associated with it and was therefore unable to be associated with a Group, but is likely of NAVZ affinity (Fig. 6).

4.2. Temporal changes in volcanic activity

While there are some data on the frequency of eruptions in the Chilean Lake District (e.g., Chaitén (Alloway et al., 2017), Villarrica and Llaima (Dzierma and Wehrmann, 2010), and Mocho-Choschuenco (Rawson et al., 2015)), relatively little is known about the frequency of eruptions from the Patagonia-Tierra del Fuego region, and particularly beyond the Holocene. This is predominantly due to a general lack of long-term records from this region.

Wastegård et al. (2013) and Naranjo and Stern (1998) report a lack of deposits from Hudson volcano in the early Holocene/Pleistocene, including proximally to the centre. However, Weller et al. (2014, 2015) identify Late Pleistocene and Early Holocene eruptions of Hudson and Carel et al. (2011) noted an abundance of Hudson deposits through both the Pleistocene and the Holocene in a marine record located to the West of the volcano. Chemical analysis of tephra layers from Laguna Potrok Aike indicates that no Hudson tephra are preserved in the Lateglacial. The only primary Hudson tephra preserved in Laguna Potrok Aike is that of H_1 at 8.7 cal ka BP (Fig. 6). The absence of primary Hudson tephra in the Laguna Potrok Aike sedimentary record possibly indicates that some of the eruptions identified by Weller et al. (2014) and Carel et al. (2011) were either smaller than H_1, and/or possibly that

wind regime and intensity has changed through the Holocene, making Hudson deposition at Laguna Potrok Aike less likely (e.g., Saunders et al., 2018). The latter is plausible since another large and widespread Hudson eruption, H_2 (4.00 ± 0.05 cal ka BP) is not identified at Laguna Potrok Aike; H_2 had a more northeasterly dispersal than H_1 (Van Daele et al., 2016).

The greatest number of volcanic deposits in the Laguna Potrok Aike record are from Mt Burney (Figs. 6 and 7), indicating that it is one of the most active volcanic centres in the Late Quaternary. There are 13 primary tephra layers of Mt Burney affinity, and 3 of these are newly identified tephra layers (LPA_12.32, 12.51, 30.15, 38.70, 40.68, 54.19, 57.03, 67.94, 72.07, 94.20 94.33, 94.96, and 95.38). These tephras are deposited across the Quaternary, between 10.2 cal ka BP (LPA_12.32) and 72.1 ka BP (LPA_95.38). Gebhardt and Ohlendorf (2019) described the sediments between 93.34 and 95.44 m-cd as a debris flow deposit. Therefore, this section was excluded from age-modelling and the age determined across this part of the sedimentary sequence is the same (~72.1 ka BP). As such the ages of the tephra units identified within this section of the sedimentary sequence, LPA_94.20, 94.33, 94.96, and 95.38, are poorly constrained since they are intercalated within a debris flow. Based on factors mentioned in Section 2.3.1, these tephras are considered to be primary (Supplementary File 2; see Section 4.3 for further information on reworking).

The longest interval without any recorded Mt Burney deposits (using average ages) is 12,740 years, between 52.6 ka (LPA_67.94) and 39.9 cal ka BP (LPA_57.03). The shortest interval is 200 years in the Holocene, between 10.2 cal ka BP (LPA_12.31) and 10.4 cal ka BP (LPA_12.51). Because Mt Burney is ~200 km from the site of Laguna Potrok Aike, it is most likely that the preserved tephra are from large, explosive events (i.e., Volcanic Explosivity Index (VEI) 5+; Newhall and Self, 1982). However, Mt Burney may well have experienced numerous smaller eruptions, which are less likely to travel sufficient distances to be preserved in the Laguna Potrok Aike sedimentary record. For example, four minor Holocene events from Mt Burney have been described by Kilian et al. (2003) and historical events have been described by Martinic (2008).

MB_1 (LPA_12.32; 10.0–10.4 cal ka BP) is preceded by a primary Mt Burney eruption only 200 years earlier, LPA_12.51 (Supplementary File 2; Fig. 4; 10.2–10.6 cal ka BP). Both deposits are chemically comparable, but distinct enough to suggest they represent two different eruptive events. LPA_12.51 is only 0.2 cm thick, while LPA_12.32 is 1.5 cm thick. LPA_12.51 could correspond to the MBK1 or MBK2 (more likely) eruption described by Kilian et al. (2003; tephra sample names: CHK7/49–51, CHK7/15–17, respectively). Previously reported ages for MBK1 and MBK2 are >8.66 ± 0.99 cal ka BP and >9.47 ± 0.06 cal ka BP, respectively (Fontijn et al., 2014; Kilian et al., 2003). Similarly, Del Carlo et al. (2018) identified a 2.5 cm thick tephra (AR-1B) of Mt Burney affinity preceding the MB_1 unit by only 2 cm of peat deposition at Arroyo Robles (51°51′S; 70°25′W).

The 1.5 cm thick LPA_18.20 Reclus eruption, commonly known as R_1, is followed soon after by LPA_21.07. LPA_21.07 is a thin, 0.3 cm thick tephra deposited at 15.7 cal ka BP, which marks the first Reclus deposit after the LGM. There is a lack of identified Reclus affinity eruptions for 47.5 kyr until the identification of LPA_77.47, LPA_77.61 and LPA_78.66, which are considered to be primary units on the basis of factors outlined in Section 2.3.1 (Supplementary File 2; See Section 4.3 for further information on reworking). It is likely that these three tephra layers were deposited relatively close to ~63.2 kyr, and that all represent very large eruptions, with LPA_78.66 being exceptionally large based on the tephra thickness (4, 8, ≥63 cm, respectively). Because much of the lithology has been classified as reworked beneath 76.50 m-cd, and is thus excluded from the age-model, it is difficult to determine the periodicity of Reclus volcanic eruptions from tephra deposits preserved in Laguna Potrok Aike (this particularly affects the determination of depositional ages for tephras from Reclus volcano identified in the lowermost sedimentary sequence). Given the thickness of the LPA_78.66 Reclus tephra in Laguna Potrok Aike (≥63 cm) at ~63.2 ka, it is likely that this unit is preserved in Antarctic and sub-Antarctic archives. The identification of this unit would be of great benefit to better understand the eruptive history of Reclus, and it could potentially allow age-transfer and the production of more robust chronologies in Antarctic and sub-Antarctic regions and thus further our understanding of Reclus event-history.

4.3. Reworking of tephra deposits

Sixty-five reworked and three likely reworked tephra layers were identified in the Laguna Potrok Aike record based on mineral componentry, glass-shard relative abundance, presence of organic and detrital material, and glass-shard morphology (Fig. 8; Supplementary File 2). As discussed, the tephra typically appears in the sequence as well-preserved, but after further inspection, is visibly reworked. In addition, there are often long periods of time and thick units of pelagic sedimentation between reworking events (Figs. 8 and 9). This strongly indicates that even visible layers that are seemingly well-preserved with distinct and sharp contacts can be reworked. If visible tephra layers can appear *in-situ* as pristine, but in fact are not, then this raises significant concerns regarding the analysis of cryptotephra (invisible ash layers) preserved in lithologies that appear to be undisturbed, for which the question of reworking is quite often overlooked. To overcome this issue in both visible and crypto-tephra studies, further respect should be given to the concept of tephra remobilisation, and detailed analysis should be undertaken on shard morphology and mineralogy, shard abundance and organic and detrital material through the entirety of the sequence.

In the case of Laguna Potrok Aike, reworked deposits are speculated to be caused predominantly by lake-basin slope instability, in addition to wind (aeolian reworking) and Quaternary lake level changes (Kliem et al., 2013a). Slope instability is possibly caused by sediment overburden on steep-sided slopes and can cause mass movement events such as debris flows or slides. Often material in debris flows is entirely disturbed (i.e., tephra unit and surrounding sediment is mixed). However, debris flows transport liquified matrix, as well as original sediment, and hence while the material in debris flows may be disturbed, slides are additionally capable of preserving complete sections of the original sedimentary sequence. In some cases, this can include fully intact tephra units and the surrounding sedimentary matrix (e.g. Sauerbrey et al., 2013). This can therefore occasionally allow for identification of a primary tephra in a section of lithology that is classified as reworked (e.g., layers LPA_77.47, 77.61 and 78.66).

Debris flows become partially diluted during advancement. This allows sediment to be brought into suspension which in turn leads to lower density of the suspension, and the production of a turbid flow (i.e., turbidite) above the debris flow (Sauerbrey et al., 2013). Turbidites differ to debris flows as they typically deposit small-scale structures that are graded from coarse to fine, and are often overlain by a clay cap (Bouma, 1965). These clay caps often contain lightweight grains such as glass-shards and organic matter which are reworked from the initial slope destabilisation and movement. Turbidites, debris flows and slides are evidenced through the Laguna Potrok Aike sedimentary sequence (e.g., Kliem et al., 2013a). Similar sedimentary processes are observed in Lake El'gygytgyn, North-eastern Siberia (Juschus et al., 2009; c. f. Sauerbrey et al., 2013). The presence of macrophytes, typically located at relatively shallow depth, in numerous samples demonstrates that tephra was

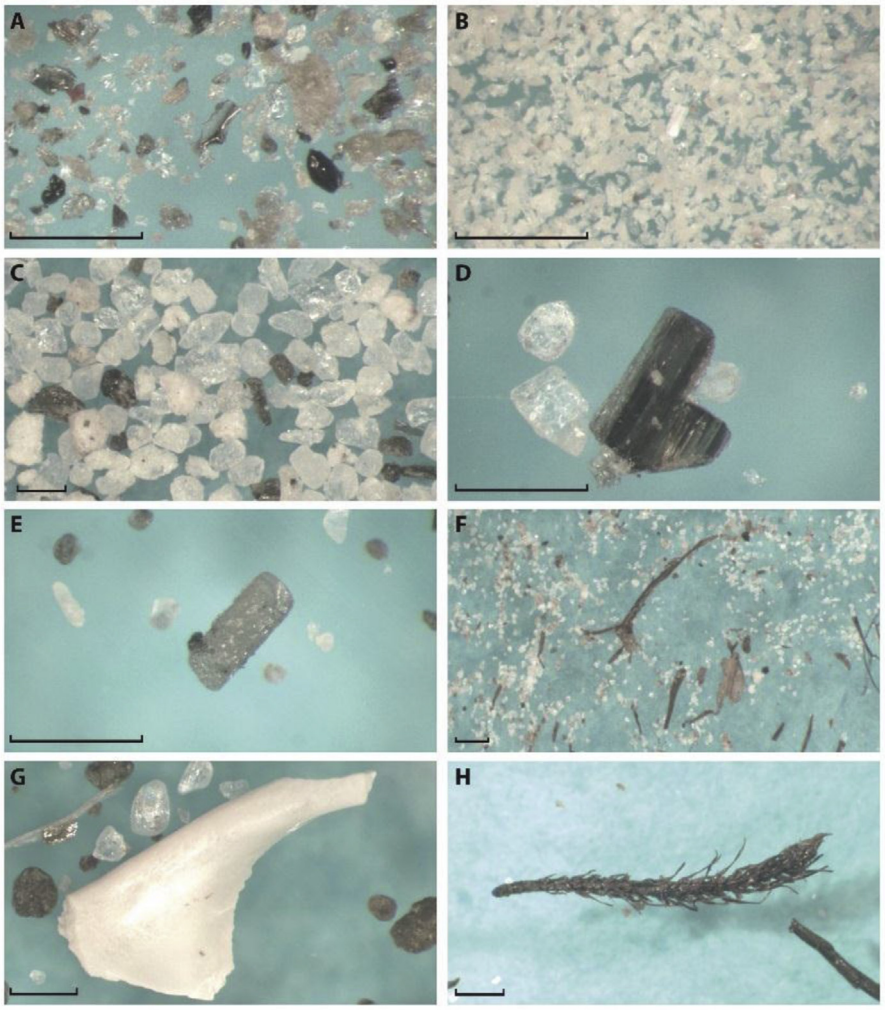

Fig. 8. Images of volcaniclastic deposits illustrate diagnostic features of primary and reworked tephra. A-D represent distinguishing features of primary tephra deposits. E-H represent distinguishing features of reworked tephra deposits. A) Fluted and vesicular shards with minimal lithics or organics (LPA_9.90; Hudson volcano, H_1); B) High relative abundance (~95%) of fluted glass shards (LPA_63.33; Lautaro/Viedma volcano); C) Low abundance of white grey pumice with high mineral abundance (~50% relative abundance; LPA_12.32, Mt Burney; MB_1); D) Angular amphibole with clear 60° cleavage plane (LPA_12.32, Mt Burney; MB_1); E) sub-rounded orthopyroxene with some glass-coating and Fe-Ti oxide (left; LPA_4.17; Hudson volcano and NAVZ); F) high proportion of organic debris (15% relative abundance of sample; LPA_16.04; Reclus volcano); G) gastropod shell fragment surrounded by rounded lithics and plagioclase (LPA_4.17; Hudson volcano and NAVZ centres); H) shoot of aquatic moss (sample is radiocarbon dated to 32.2 cal ka BP; LPA_47.86; insufficient chemical data to identify source). Scale bars (total lengths: 50 μm) are presented for individual photos in the bottom left corner.

moved rapidly to deeper parts of the lake, and is indicative of reworking produced by either sediment destabilisation or lake-level changes (e.g., Jouve et al., 2017).

Three Holocene tephra layers (LPA_11.71, 12.16, and 21.07) in the sequence are reworked but have no affiliated primary tephra unit. It is hypothesised that these tephra layers, and possibly others, were deposited by aeolian reworking. Here, we speculate that primary tephra was deposited away from the lake, and that these layers were resuspended via wind (notably the strong and dominating Southern Westerly Winds) very soon after or during deposition, resulting in (reworked) tephra layer formation in the Laguna Potrok Aike sedimentary sequence (e.g., Bertrand et al., 2014). This mechanism is particularly considered in the case of thin reworked units identified, and provides some explanation for the identification of rounded minerals and lack of glass-shard abundances in some layers.

The capability of already deposited tephra to be remobilised by wind was observed after the 1991 eruption of Hudson volcano (VEI 5), whereby strong winds caused ash to be remobilised and identified >1000 km from source, across Argentina and the western Atlantic Ocean (Wilson et al., 2011). Zanchetta et al. (2018) also documented aeolian redistribution of Lateglacial H_o tephra from Hudson volcano across Argentina, >400 km to the southeast of the main axis of the H_o tephra distribution. Fowler and Lopushinsky (1986) identified that even low wind speeds of 6–9 km/h^{-1} (1.6–2.5 m s^{-1}) are capable of mobilising unconsolidated tephra; in the Pali Aike region, wind speeds are known to reach averages of 28.8 km/h^{-1} (8 m s^{-1}; Ohlendorf et al., 2013), indicating the great potential for unconsolidated tephra to be remobilised by wind in the study region. Additionally, Monteath et al. (2019) has associated cryptotephra layers with heterogeneous chemistry from Southern South America, identified in Hookers Point, Falkland Islands, as reworked by wind. They attributed temporal patterns of abundant reworked volcanic glass with changes in the position and/or strength of the Southern Westerly Winds (Monteath et al., 2019). Layers deposited by wind may provide scope to further understand the frequency of volcanic events, as well as dust influx from southernmost South America. However, owing to the high number

of reworked layers in the Laguna Potrok Aike sedimentary record, reworked layers have been excluded from frequency analysis.

Reworked tephra layers are finally also thought to possibly result from lake-level changes which caused tephra mobilisation and erosion (e.g., Jouve et al., 2017). During the Holocene, South America experienced variable climatic conditions (e.g., Markgraf et al., 2003) which may have contributed to lake level changes, and certainly, Holocene palaeoshorelines have been identified for

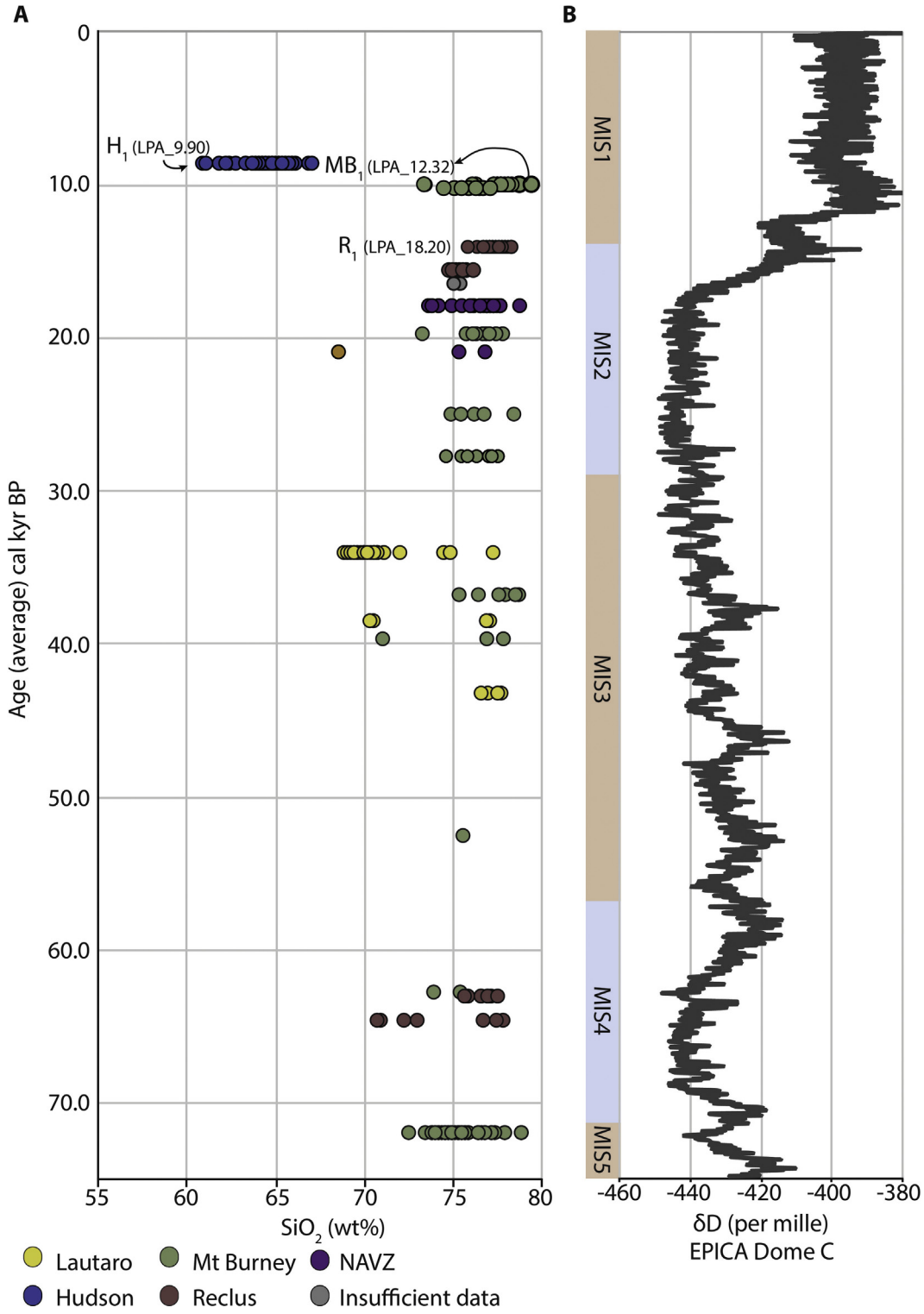

Fig. 9. Plenary diagram for temporal changes in tephra chemistry. A) Tephra chemistry for primary (solid circles with black outline) deposits in the lake sequence – colours relate to the source of the deposit; See Supplementary File 2 for further information; B) Deuterium (δD) data from Antarctic ice core Epica Dome C after Jouzel (2004). Marine Isotope Stages (MIS) are marked and reflect stadial/glacial (even numbers) and interstadial/interglacial (odd numbers) conditions (after Lisiecki and Raymo, 2005). (For interpretation of the references to colour in this figure legend, the reader is referred to the Web version of this article.)

Laguna Potrok Aike (Anselmetti et al., 2009; Haberzettl et al., 2007; Kliem et al., 2013b). It is thus hypothesised that changes in lake levels are a suitable explanation for the repetitive reworking of tephra deposits between 8.7 cal ka BP and the present day. During the Lateglacial, lake level at Laguna Potrok Aike is thought to have been relatively stable (e.g., Anselmetti et al., 2009; Haberzettl et al., 2007; Zolitschka et al., 2013); the identification of numerous reworked layers during this time period therefore indicates that other reworking processes (i.e., wind, lake basin instability) are more dominant at this time.

4.4. Changes in eruptive activity in relation to climate

There are limited records of long-term climate change in southern South America because of the advance and retreat of the Patagonian Ice Sheet (e.g., Fontijn et al., 2014). As such, Antarctic ice cores are thought to proffer the most representative record of climate change for the study region beyond the Lateglacial. The volcanic record from Laguna Potrok Aike is analysed with respect to climatological data derived from ice cores to determine if any relationship exists between volcanic activity and ice-unloading (Fig. 9). This relationship has been discussed in Rawson et al. (2016) and Watt et al. (2013) but in these studies only the Holocene is accounted for.

Ice sheets were particularly thick and extensive during MIS 4 (57–71 ka BP; Lisiecki and Raymo, 2005) in southern South America (Clapperton, 1994; Kaplan et al., 2008), and between ~53 and 65 ka BP (MIS3/MIS4), there was a decline in insolation at 40°S (Van Meerbeeck et al., 2009). This period coincides with a decline in eruptive activity recorded for Laguna Potrok Aike; between 62.9 and 43.4 cal ka BP (LPA_72.07 and 63.33, respectively) only one eruptive deposit is identified (LPA_67.94; Fig. 9).

It is possible that the lack of volcanic deposits identified between 62.9 and 43.4 cal ka BP is a consequence of ice-overburden on volcanic centres, and that the effect of this ice-overburden inhibited eruptive activity (e.g., Jellinek et al., 2004; Rawson et al., 2016; Watt et al., 2013). Alternatively, the lack of identified volcanic deposits in the lake during this time may reflect a lack of preserved (visible) deposits rather than a decline in overall volcanic activity, which may be caused for example, by different dominant wind directions. It is, however, difficult to speculate with no other long term records of such high resolution.

5. Conclusions

This detailed investigation of tephra preserved in the Laguna Potrok Aike sedimentary record provides the fullest account to date of eruptive activity in southern South America over the last 80 kyr.

- Correlations to source volcanoes are based on a newly established database of glass-geochemistry from proximal deposits of regionally distributed eruptions: A_1, R_1, MB_1, MB_2, H_1, and H_2, in addition to the tephra chemistry of widespread deposits described in Del Carlo et al. (2018) and Mayr et al. (2019). Three previously known regional marker horizons are now better chemically and chronologically characterised: H_1 (Hudson), identified in the PASADO record for the first time, has a depositional age of 8.6–9.0 cal ka BP; MB_1 has a depositional age of 10.0–10.4 cal ka BP, and R_1 has a depositional age of ~14.1–14.5 cal ka BP.
- We have built on previous tephra studies by Kliem et al. (2013a) and Wastegård et al. (2013). From this research we have identified nine new primary tephra layers. The chemical affinity of all layers from the Laguna Potrok Aike sedimentary record is presented for the first time.
- There are 94 visible tephra units preserved in the sedimentary sequence of Laguna Potrok Aike. Twenty-five of these have been emplaced by primary fallout, but 65 are reworked, 3 are likely reworked, and insufficient information is available for 1 layer. These reworked layers appear primary but have characteristic features of reworking based on microscopic and geochemical analysis. This strongly indicates that even well-preserved visible tephra in sedimentary archives may not be primary. As such, special care must be taken in the analysis of both visible, and (especially) invisible (crypto-) tephra layers to decipher their emplacement mechanisms; this includes visual inspection of the glass, and their chemical composition. In the case of invisible tephra in sediments which appear undisturbed, this should include a thorough study of changing shard morphological properties throughout the sequence to determine background changes from true eruptive events (e.g., McLean et al., 2018). The relocation of a widespread marker horizon in a sequence with numerous, very obvious visible tephra layers (Figs. 8 and 9) demonstrates that reworking of tephra is undoubtedly more prevalent in (at least) lacustrine records than currently appreciated. Further work should include the development of a standardised framework of glass-shard inspection for reworked deposits in different environments.
- There is a period of very low eruptive activity in the region recorded between 62.9 and 43.4 cal ka BP. At present it cannot be established whether this period reflects reduced eruptive activity or reduced preservation. As such, it is difficult to determine whether there is a relationship between climate and volcanism in this study region with only a single record.
- Further work should involve renewed efforts, using internationally recognised methods of tephra identification and analysis, to fingerprint these widespread marker horizons in extra-Andean records, including Antarctic ice-cores which are excellent archives of tephra on long time-scales. Such work would further inform on the scale of southern South American eruptive activity beyond the Lateglacial.

Acknowledgements

RS is funded by NERC as part of the Environmental Research Doctoral Training Partnership at the University of Oxford (grant: NE/L002621/1). KF was supported by NERC large grant NE/L013932/1 (Rift Volcanism: Past, Present and Future). This research was supported by the International Continental Scientific Drilling Program (ICDP) in the framework of the "Potrok Aike Maar Lake Sediment Archive Drilling Project" (PASADO). Funding for drilling was provided by the ICDP, the German Science Foundation (DFG), the Swiss National Funds (SNF), the Natural Sciences and Engineering Research Council of Canada (NSERC), the Swedish Vetenskapsrådet (VR) and the University of Bremen. CM acknowledges financial support by BMBF (01DN16025). For their invaluable help in field logistics, we thank: the staff of INTA Santa Cruz, Rio Dulce Catering, as well as the Moreteau family, and for drilling: the DOSECC crew. The authors would like to thank Alessio Di Roberto and an anonymous reviewer for their invaluable comments.

Appendix A. Supplementary data

Supplementary data to this article can be found online at https://doi.org/10.1016/j.quascirev.2019.06.001.

References

Alloway, B.V., Pearce, N.J.G., Moreno, P.I., Villarosa, G., Jara, I., De Pol-Holz, R., Outes, V., 2017. An 18,000 year-long eruptive record from Volcán Chaitén,

northwestern Patagonia: paleoenvironmental and hazard-assessment implications. Quat. Sci. Rev. 168, 151–181.
Anselmetti, F.S., Ariztegui, D., De Batist, M., Gebhardt, A.C., Haberzettl, T., Niessen, F., Ohlendorf, C., Zolitschka, B., 2009. Environmental history of southern Patagonia unravelled by the seismic stratigraphy of Laguna Potrok Aike. Sedimentology 56, 873–892.
Bendle, J.M., Palmer, A.P., Thorndycraft, V.R., Matthews, I.P., 2017. High-resolution chronology for deglaciation of the patagonian ice sheet at Lago Buenos Aires (46.5 °S) revealed through varve chronology and Bayesian age modelling. Quat. Sci. Rev. 177, 314–339. https://doi.org/10.1016/j.quascirev.2017.10.013.
Bertrand, S., Daga, R., Bedert, R., Fontijn, K., 2014. Deposition of the 2011-2012 Cordón Caulle tephra (Chile, 40S) in lake sediments: implications for tephrochronology and volcanology. J. Geophys. Res. F Earth Surface 119, 2555–2573.
Blockley, S.P.E., Pyne-O'Donnell, S.D.F., Lowe, J.J., Matthews, I.P., Stone, A., Pollard, A.M., Turney, C.S.M., Molyneux, E.G., 2005. A new and less destructive laboratory procedure for the physical separation of distal glass tephra shards from sediments. Quat. Sci. Rev. 24, 1952–1960.
Bouma, A., 1965. Sedimentary characteristics of samples collected from submarine canyons. Mar. Geol. 3, 291–320.
Carel, M., Siani, G., Delpech, G., 2011. Tephrostratigraphy of a deep-sea sediment sequence off the south Chilean margin: new insight into the Hudson volcanic activity since the last glacial period. J. Volcanol. Geotherm. Res. 208, 99–111.
Clapperton, C.M., 1994. The quaternary glaciation of Chile : a review. Rev. Chil. Hist. Nat. 67, 369–383.
Coronato, A., Ercolano, B., Corbella, H., Tiberi, P., 2013. Glacial, fluvial and volcanic landscape evolution in the Laguna Potrok Aike maar area, Southern Patagonia, Argentina. Quat. Sci. Rev. 71, 13–26.
Crowley, J.W., Katz, R.F., Huybers, P., Langmuir, C.H., Park, S., 2015. Glacial cycles drive variations in the production of oceanic crust. Science 347, 1237–1240.
Del Carlo, P., Di Roberto, A., D'Orazio, M., Petrelli, M., Angioletti, A., Zanchetta, G., Maggi, V., Daga, R., Nazzari, M., Rocchi, S., 2018. Late Glacial-Holocene tephra from southern Patagonia and Tierra del Fuego (Argentina, Chile): a complete textural and geochemical fingerprinting for distal correlations in the Southern Hemisphere. Quat. Sci. Rev. 195, 153–170.
Dzierma, Y., Wehrmann, H., 2010. Eruption time series statistically examined: probabilities of future eruptions at Villarrica and Llaima volcanoes, southern volcanic zone, Chile. J. Volcanol. Geotherm. Res. 193, 82–92.
Fontijn, K., Lachowycz, S.M., Rawson, H., Pyle, D.M., Mather, T.A., Naranjo, J.A., Moreno-Roa, H., 2014. Late Quaternary tephrostratigraphy of southern Chile and Argentina. Quat. Sci. Rev. 89, 70–84.
Fontijn, K., Rawson, H., Van Daele, M., Moernaut, J., Abarzúa, A.M., Heirman, K., Bertrand, S., Pyle, D.M., Mather, T.A., De Batist, M., Naranjo, J.-A., Moreno, H., 2016. Synchronisation of sedimentary records using tephra: a postglacial tephrochronological model for the Chilean Lake District. Quat. Sci. Rev. 137, 234–254.
Fowler, W.B., Lopushinsky, W., 1986. Wind-blown volcanic ash in forest and agricultural locations as related to meteorological conditions. Atmos. Environ. 20, 421–425.
Gebhardt, C., Ohlendorf, C., 2019. Revised Age Model for Composite Core 5022-2CP, Laguna Potrok Aike, Patagonia. PANGAEA. https://doi.pangaea.de/10.1594/PANGAEA.901831.
Haberzettl, T., Corbella, H., Fey, M., Janssen, S., Lücke, A., Mayr, C., Ohlendorf, C., Schäbitz, F., Schleser, G.H., Wille, M., Wulf, S., Zolitschka, B., 2007. Lateglacial and Holocene wet-dry cycles in southern Patagonia: chronology, sedimentology and geochemistry of a lacustrine record from Laguna Potrok Aike, Argentina. Holocene 17, 297–310.
Huybers, P., Langmuir, C., 2009. Feedback between deglaciation, volcanism, and atmospheric CO2. Earth Planet. Sci. Lett. 286, 479–491.
Jellinek, A.M., Manga, M., Saar, M.O., 2004. Did melting glaciers cause volcanic eruptions in eastern California? Probing the mechanics of dike formation. J. Geophys. Res. B Solid Earth 109, 1–10.
Jochum, K.P., Stoll, B., Herwig, K., Willbold, M., Hofmiann, A.W., Amini, M., Aarburg, S., Abouchami, W., Hellebrand, E., Mocek, B., Raczek, I., Stracke, A., Alard, O., Bouman, C., Becker, S., Dücking, M., Brätz, H., Klemd, R., De Bruin, D., Canil, D., Cornell, D., De Hoog, C.J., Dalpé, C., Danyushevshy, L., Eisenhauer, A., Gao, Y., Snow, J.E., Groschopf, N., Günther, D., Latkoczy, C., Guillong, M., Hauri, E.H., Höfer, H.E., Lahaye, Y., Horz, K., Jacob, D.E., Kasemann, S.A., Kent, A.J.R., Ludwig, T., Zack, T., Mason, P.R.D., Meixner, A., Rosner, M., Misawa, K., Nash, B.P., Pfänder, J., Premo, W.R., Sun, W.D., Tiepolo, M., Vannucci, R., Vennemann, T., Wayne, D., Woodhead, J.D., 2006. MPI-DING reference glasses for in situ microanalysis: new reference values for element concentrations and isotope ratios. Geochem. Geophys. Geosyst. 7 (2), Q02008. https://doi.org/10.1029/2005GC001060.
Jouve, G., Lisé-Pronovost, A., Francus, P., De Coninck, A.S., 2017. Climatic influence of the latest Antarctic isotope maximum of the last glacial period (AIM4) on Southern Patagonia. Palaeogeogr. Palaeoclimatol. Palaeoecol. 472.
Jouzel, J., 2004. EPICA Dome C Ice Cores Deuterium Data. IGBP PAGES, World Data Center for Paleoclimatology, Data Contribution Series #2004-038. NOAA/NGDC Paleoclimatology Program, Boulder CO, USA.
Jull, M., McKenzie, D., 1996. The effect of deglaciation on mantle melting beneath Iceland. J. Geophys. Res. 101 (21), 815–821, 828.
Juschus, O., Melles, M., Gebhardt, A.C., Niessen, F., 2009. Late quaternary mass movement events in lake El'gygytgyn, north-eastern Siberia. Sedimentology 56, 2155–2174.
Kaplan, M.R., Moreno, P.I., Rojas, M., 2008. Glacial dynamics in southernmost South America during marine isotope stage 5e to the Younger Dryas chron: a brief review with a focus on cosmogenic nuclide measurements. J. Quat. Sci. 23, 649–658.
Kilian, R., Hohner, M., Biester, H., Wallrabe-Adams, H.J., Stern, C.R., 2003. Holocene peat and lake sediment tephra record from the southernmost Chilean Andes (53-55°S). Rev. Geol. Chile 30, 1–17.
Kliem, P., Enters, D., Hahn, A., Ohlendorf, C., Lisé-Pronovost, A., St-Onge, G., Wastegård, S., Zolitschka, B., 2013a. Lithology, radiocarbon chronology and sedimentological interpretation of the lacustrine record from Laguna Potrok Aike, southern Patagonia. Quat. Sci. Rev. 71, 54–69.
Kliem, P., Buylaert, J.P., Hahn, A., Mayr, C., Murray, A.S., Ohlendorf, C., Veres, D., Wastegård, S., Zolitschka, B., 2013b. Magnitude, geomorphologic response and climate links of lake level oscillations at Laguna Potrok Aike, Patagonian steppe (Argentina). Quat. Sci. Rev. 71, 131–146.
Koffman, B.G., Dowd, E.G., Osterberg, E.C., Ferris, D.G., Hartman, L.H., Wheatley, S.D., Kurbatov, A.V., Wong, G.J., Markle, B.R., Dunbar, N.W., Kreutz, K.J., Yates, M., 2017. Rapid transport of ash and sulfate from the 2011 Puyehue-Cordón Caulle (Chile) eruption to West Antarctica. J. Geophys. Res. Atmos. 122, 8908–8920.
Lisiecki, L., Raymo, M., 2005. A Pliocene-Pleistocene stack of 57 globally distributed Benthic δ180 records. Palaeoceanography 20, PA1003.
Lowe, D.J., 2011. Tephrochronology and its application: a review. Quat. Geochronol. 6, 107–153.
Markgraf, V., Bradbury, J., Schwalb, A., Burns, S., Stern, C., Ariztegui, D., Gilli, A., Anselmetti, F., Stine, S., Maidana, N., 2003. Holocene palaeoclimates of southern Patagonia: limnological and environmental history of Lago Cardiel, Argentina. Holocene 13, 581.
Martinic, M., 2008. Registro historico de antecedentes volcánicos y sísmicos en la Patagonia Austral y la Tierra del Fuego. Magallania 36, 5–18.
Massone, M., 1989. Investigaciones arqueologicas en la laguna Thomas Gold. An. Inst. Patagon 19, 87–99.
Mayr, C., Smith, R.E., García, M.L., Massaferro, J., Lücke, A., Dubois, N., Maidana, N.I., Meier, W.J.-H., Wissel, H., Zolitschka, B., 2019. Historical eruptions of Lautaro volcano and their impacts on lacustrine ecosystems in southern Argentina. J. Palaeolimnology. https://doi.org/10.1007/s10933-019-00088-y.
McLean, D., Albert, P.G., Nakagawa, T., Suzuki, T., Staff, R.A., Yamada, K., Kitaba, I., Haraguchi, T., Kitagawa, J., Smith, V., 2018. Integrating the Holocene tephrostratigraphy for East Asia using a high-resolution cryptotephra study from Lake Suigetsu (SG14 core), central Japan. Quat. Sci. Rev. 183, 36–58.
Monteath, A., Hughes, P.D.M., Wastegård, S., 2019. Evidence for distal transport of reworked Andean tephra: extending the cryptotephra framework from the Austral Volcanic Zone. Quat. Geochronol. 51, 64–71. https://doi.org/10.1016/j.quageo.2019.01.003.
Naranjo, J.A., Stern, C.R., 1998. Holocene explosive activity of Hudson volcano, southern Andes. Bull. Volcanol. 59, 291–306.
Naranjo, J.A., Stern, C.R., 2004. Holocene tephrochronology of the southernmost part (42°30'-45°S) of the Andean southern volcanic zone. Rev. Geol. Chile 31, 224–240.
Narcisi, B., Petit, J.R., Delmonte, B., Scarchilli, C., Stenni, B., 2012. A 16,000-yr tephra framework for the Antarctic ice sheet: a contribution from the new Talos Dome core. Quat. Sci. Rev. 49, 52–63.
Newhall, C.G., Self, S., 1982. The volcanic explosivity index (VEI): an estimate of explosive magnitude for historical volcanism. J. Geophys. Res.: Atmos. 87, 1231–1238.
Nowell, D.A.G., Jones, M.C., Pyle, D.M., 2006. Episodic quaternary volcanism in France and Germany. J. Quat. Sci. 21, 645–675.
Ohlendorf, C., Fey, M., Gebhardt, C., Haberzettl, T., Lücke, A., Mayr, C., Schäbitz, F., Wille, M., Zolitschka, B., 2013. Mechanisms of lake-level change at Laguna Potrok Aike (Argentina) - insights from hydrological balance calculations. Quat. Sci. Rev. 71, 27–45.
Oppedal, L.T., van der Bilt, W.G.M., Balascio, N.L., Bakke, J., 2018. Patagonian ash on sub-Antarctic South Georgia: expanding the tephrostratigraphy of southern South America into the Atlantic sector of the Southern Ocean. J. Quat. Sci. 33 (5), 482–486.
Pearce, N.J.G., 2014. Towards a protocol for the trace element analysis of glass from rhyolitic shards in tephra deposits by laser ablation ICP-MS. J. Quat. Sci. 29, 627–640.
Prieto, A., Stern, C.R., Estévez, J.E., 2013. The peopling of the Fuego-Patagonian fjords by littoral hunter-gatherers after the mid-Holocene H1 eruption of Hudson Volcano. Quat. Int. 317, 3–13.
Rawson, H., Naranjo, J.A., Smith, V.C., Fontijn, K., Pyle, D.M., Mather, T.A., Moreno, H., 2015. The frequency and magnitude of post-glacial explosive eruptions at Volcán Mocho-Choshuenco, southern Chile. J. Volcanol. Geotherm. Res. 299, 103–129.
Rawson, H., Pyle, D.M., Mather, T.A., Smith, V.C., Fontijn, K., Lachowycz, S.M., Naranjo, J.A., 2016. The magmatic and eruptive response of arc volcanoes to deglaciation: insights from southern Chile. Geology 44, 251–254.
Shane, P., 2000. Tephrochronology: a New Zealand case study. Earth Sci. Rev. 49, 223–259.
Sauerbrey, M.A., Juschus, O., Gebhardt, A.C., Wennrich, V., Nowaczyk, N.R., Melles, M., 2013. Mass movement deposits in the 3.6 Ma sediment record of Lake El'gygytgyn, far east Russian Arctic. Clim. Past 9, 1949–1967.
Saunders, K.M., Roberts, S.J., Perren, B., Butz, C., Sime, L., Davies, S., Van Nieuwenhuyze, W., Grosjean, M., Hodgson, D.A., 2018. Holocene dynamics of the Southern Hemisphere westerly winds and possible links to CO2 outgassing. Nat. Geosci. 11, 650–655.

Sigvaldason, G., Annertz, K., Nilsson, M., 1992. Effect of glacier loading/deloading on volcanism: postglacial volcanic production rate of the Dyngjufjöll area, central Iceland. Bull. Volcanol. 54, 385–392.
Stern, C.R., 1992. Tefrocronologia de Magallanes: nuevos datos e implicaciones. Anales del Insituto de la Patagonia 21, 129–141.
Stern, C.R., 2004. Active Andean volcanism: its geologic and tectonic setting. Rev. Geol. Chile 31, 1–51.
Stern, C.R., 2008. Holocene tephrochronology record of large explosive eruptions in the southernmost Patagonian Andes. Bull. Volcanol. 70, 435–454.
Stern, C.R., De Porras, M.E., Maldonado, A., 2015. Tephrochronology of the upper Rio Cisnes valley (44°S), southern Chile. Andean Geol. 42, 173–189.
Stern, C.R., Moreno, P.I., Henríquez, W.I., Villa-Martínez, R., Sagredo, E., Aravena, J.C., 2016. Tephrochronology of the area around Cochrane, southern Chile. Andean Geol. 43 (1), 1–19.
Stern, C.R., Moreno, P.I., Villa-Martínez, R., Sagredo, E.A., Prieto, A., Labarca, R., 2011. Evolution of ice-dammed proglacial lakes in Última Esperanza, Chile: implications from the late-glacial R1 eruption of Reclús volcano, Andean Austral Volcanic Zone. Andean Geol. 38, 82–97.
Strelin, J.A., Malagnino, E.C., 2000. Late-glacial history of Lago Argentino, Argentina, and age of the puerto bandera Moraines. Quat. Res. 54, 339–347.
Terry, R.,D., Chilingar, G.,V., 1955. Summary of 'Concerning some additional aids in studying sedimentary formations' by Shvestsov, MS. J. Sediment. Petrol. 25, 3.
Tomlinson, E.L., Smith, V.C., Albert, P.G., Aydar, E., Civetta, L., Cioni, R., Çubukçu, E., Gertisser, R., Isaia, R., Menzies, M.A., Orsi, G., Rosi, M., Zanchetta, G., 2015. The major and trace element glass compositions of the productive Mediterranean volcanic sources: tools for correlating distal tephra layers in and around Europe. Quat. Sci. Rev. 118, 48–66.
Tomlinson, E.L., Thordarson, T., Müller, W., Thirlwall, M., Menzies, M.A., 2010. Microanalysis of tephra by LA-ICP-MS - strategies, advantages and limitations assessed using the Thorsmörk ignimbrite (Southern Iceland). Chem. Geol. 279, 73–89.
Van Daele, M., Bertrand, S., Meyer, I., Moernaut, J., Vandoorne, W., Siani, G., Tanghe, N., Ghazoui, Z., Pino, M., Urrutia, R., Batist, M. De, 2016. Late Quaternary evolution of Lago Castor (Chile, 45.6°S): timing of the deglaciation in northern Patagonia and evolution of the southern westerlies during the last 17 kyr. Quat. Sci. Rev. 133, 130–146.
Van Meerbeeck, C.J., Renssen, H., Roche, D.M., 2009. How did marine isotope stage 3 and last glacial maximum climates differ? - perspectives from equilibrium simulations. Clim. Past 5, 33–51.
Villa-Martinez, R., Moreno, P.I., 2007. Pollen evidence for variations in the southern margin of the westerly winds in SW Patagonia over the last 12,600 years. Quat. Res. 68, 400–409.
Wastegård, S., Veres, D., Kliem, P., Hahn, a., Ohlendorf, C., Zolitschka, B., 2013. Towards a late Quaternary tephrochronological framework for the southernmost part of South America - the Laguna Potrok Aike tephra record. Quat. Sci. Rev. 71, 81–90.
Watt, S.F.L., Pyle, D.M., Mather, T.A., 2013. The volcanic response to deglaciation: evidence from glaciated arcs and a reassessment of global eruption records. Earth Sci. Rev. 122, 77–102.
Weller, D.J., Miranda, C.G., Moreno, P.I., Villa- Martínez, R., Stern, C.R., 2015. Tephrochronology of the southernmost Andean southern volcanic zone, Chile. Bull. Volcanol. 77, 1–24.
Weller, D.J., Miranda, C.G., Moreno, P.I., Villa-Martínez, R., Stern, C.R., 2014. The large late-glacial Ho eruption of the Hudson volcano, southern Chile. Bull. Volcanol. 76, 1–18.
Weller, D.J., Porras, M.E., De Maldonado, A., Mendez, C., Stern, C.R., 2017. Holocene tephrochronology of the lower Río Cisnes valley, southern Chile. Andean Geol. 44, 229–248.
Weller, D.J., Porras, M. E. De, Maldonado, A., Mendez, C., Stern, C.R., 2018. New age controls on the tephrochronology of the southernmost Andean southern volcanic zone, Chile. Quat. Res. 91 (1), 1–5. https://doi.org/10.1017/qua.2018.81.
Weller, D.J., Porras, M. E. De, Maldonado, A., Mendez, C., Stern, C.R., 2019. Petrology, geochemistry and correlation of tephra deposits from a large early Holocene eruption of Mentolat volcano, southern Chile. J. South Am. Earth Sci. 90, 282–285.
Wilson, T.M., Cole, J.W., Stewart, C., Cronin, S.J., Johnston, D.M., 2011. Ash storms: impacts of wind-remobilised volcanic ash on rural communities and agriculture following the 1991 Hudson eruption, southern Patagonia, Chile. Bull. Volcanol. 73, 223–239.
Zanchetta, G., Ribolini, A., Ferrari, M., Bini, M., Isola, I., Lezzerini, M., Baroni, C., Salvatore, M.C., Pappalardo, M., Fucks, E., Boretto, G., 2018. Geochemical characteristics of the infilling of ground wedges at puerto deseado (Santa Cruz, Argentina): palaeoenvironmental and chronological implications. Andean Geol. 45, 130–144.
Zolitschka, B., Anselmetti, F., Ariztegui, D., Corbella, H., Francus, P., Lücke, A., Maidana, N.I., Ohlendorf, C., Schäbitz, F., Wastegård, S., 2013. Environment and climate of the last 51,000 years - new insights from the Potrok Aike maar lake Sediment Archive Drilling prOject (PASADO). Quat. Sci. Rev. 71, 1–12.
Zolitschka, B., Corbella, H., Maidana, N., Ohlendorf, C., 2006. Investigating maar formation and the climate history of southern Argentina - the Potrok Aike Maar Lake sediment archive drilling Project (PASADO). Sci. Drill. 3, 54–55. https://doi.org/10.2204/iodp.sd.3.13.2006.